SOLVENT EXTRACTION BY A RISING SLUG

SOLVENT EXTRACTION BY A RISING SLUG

By

MAN KEI HO, B.Sc.

A Project Report

Submitted to the School of Graduate Studies

in Partial Fulfilment of the Requirements

for the Degree

Master of Engineering

McMaster University

Septmember 1978

MASTER OF ENGINEERING (1978) McMaster University
(Chemical Engineering) Hamilton, Ontario

TITLE : Solvent extraction by a rising slug

AUTHOR : Man Kei Ho, B.Sc. (University of Alberta)

SUPERVISOR : Professor M.H.I. Baird

NUMBER OF PAGES : viii, 102

ABSTRACT

Several types of apparatus have been previously developed to give a constant and measurable interfacial area for solvent extraction. In this work, a new and relatively simple device for this purpose has been tested. The organic phase is allowed to rise or fall freely through the aqueous phase in a tube as a cylindrical "slug". In the mass transfer operation, the "slug" of sparingly-soluble organic liquid is held stationary by the downflow of water. The shrinkage rate of the slug can be measured easily and it gives the experimental mass transfer rate. In order to apply the Higbie penetration theory to the experimental conditions, the interfacial velocity and radius ratio of the slug must be known; these factors can be calculated from the hydrodynamics of the system, using the measured value of slug superficial velocity. Finally, a comparison between experimental and theoretical mass transfer results can be made. 1-butanol shows a good agreement (to within 1%) while 1-pentanol and methyl iso-butyl ketone show less satisfactory agreement due to lack of precise data on their molecular diffusivities in water.

ACKNOWLEDGEMENTS

I sincerely thank the supervision and interest of Dr. M.H.I. Baird during the experimental program and the preparation of this report.

TABLE OF CONTENTS

LIST OF TABLES

LIST OF FIGURES

1. INTRODUCTION

Fundamental kinetics studies on solvent extraction are normally carried out with a constant and measurable interfacial area. If both interfacial area and concentration driving force are known, with the mass transfer rate measured, the overall mass transfer coefficient can be obtained.

It is useful to be able to predict the mass transfer coefficient from first principles; the prediction can then be compared with experimental values. In the presence of chemical reaction, the situation would be very complicated because it involves the determination of the rate controlling step. Therefore, for simplicity, only physical interfacial transport is considered in this work.

There are several types of apparatus that give a constant and measurable interfacial area in gas-liquid systems and have been found successful in giving predictable mass transfer rates by using the Higbie Penetration Theory[1]:

1. The rotating drum: This apparatus was used by Danckwerts and Kennedy[2](1954). It was a 10 cm diameter drum partly immersed in the liquid and it carried a film of liquid as it rotated.
2. The wetted-wall column: In this type of apparatus, the

liquid flows in a film, under the influence of gravity, down a surface which is usually a vertical tube or a rod with gas flowing countercurrently or cocurrently. An example of these wetted-wall columns was described by Roberts and Danckwerts[3](1962).

3. The laminar jet: A jet of liquid enters the gas-space through a circular orifice, and leaves through a slightly larger hole. This device was used by Scriven and Pigford[4] (1958), among others.
4. The wetted sphere: This apparatus was first used by Lynn et al.[5](1955). The absorbent liquid flowed over the surface of a sphere in a laminar film.
5. The moving-band: In this apparatus, constructed by Govindan and Quinn[6](1964), an endless band of nichrome ribbon passes through the gas carrying on its surface a film of liquid.

Several attempts have also been made to adapt the same types of apparatus to liquid-liquid systems; Ward and Quinn[7] used jets, Ratcliff and Reid[8] used wetted spheres and Bakker et al.[9] used wetted-wall columns.

In this work, a device which is rather like a wetted-wall column but basically much simpler has been developed. The organic phase is allowed to rise or fall freely through the aqueous phase in a tube as a cylindrical "slug". It is important that the tube wall is preferentially wetted by the aqueous phase. Glass is excellent for

this purpose and of course has the advantage that it can be chemically cleaned by chromic acid.

A smooth stable slug interface is obtained when the slug flow is laminar, and this can be achieved by having the tube diameter slightly greater than the critical diameter for the system. The critical diameter is the diameter at and below which slug flow is prevented by capillary effects.

In order to apply the penetration theory, the contact time τ and interfacial area must be known, where the contact time τ is the slug length divided by interfacial velocity. The slug length is easily measured, but the radius of the slug and the interfacial velocity must be estimated from the hydrodynamics of the system. Then a comparison can be made between Higbie penetration theory and experimentally measured rates of mass transfer.

The objectives of this project are the evaluation of the slug technique and the experimental confirmation of the mass transfer theory for several liquid-liquid systems.

2. EXPERIMENTAL APPARATUS AND PROCEDURES

2.1. Rising slug without mass transfer

Initial measurements were carried out to determine the rise velocity and stability of slugs in the absence of mass transfer. The apparatus for the rising slug measurement which is illustrated in figure 1 was a 100 cm glass tube. Seven internal tube diameters were employed in the experiment: 4.08 ,6.04 ,8.16 ,9.80 ,11.53 ,14.69, 18.99 mm . Kerosene(odorless), Benzene, 1-Butanol and Carbon Tetrachoride were taken as the organic phases in the experiments. In order to prevent mass transfer during the velocity measurements, all four organic liquids were first saturated with water. Each organic liquid was poured into a 500 mL separation flask and water was then added. The flask was stoppered and then shaken vigorously for several minutes. Sometimes the time taken would be longer, it all depended on the amounts of the liquids inside the flask.

One end of the glass tube was stoppered, and then mutually saturated water was poured into it leaving a few centimeters empty at the top. The saturated organic liquid was pipetted from the flask and drained into the glass tube which had been nearly filled up by mutually saturated water. When the organic liquid overflowed, the open end was stoppered in such a way that no air bubble was trapped inside

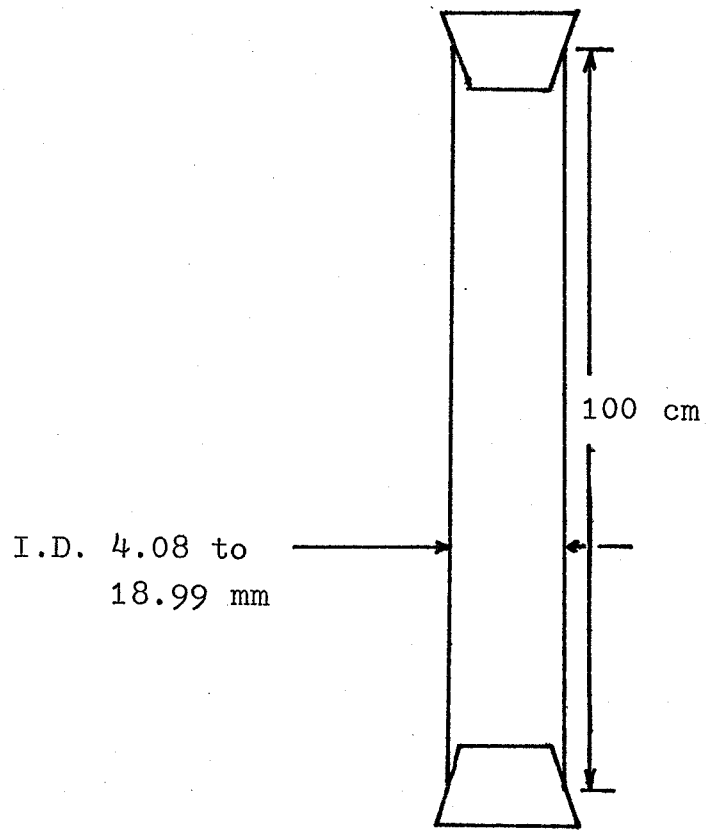

Figure 1. 100 cm glass tube with stoppers, used in rising-slug experiments

the tube. The length of the stationary slug was measured by a transparent ruler. Three different slug length rising velocities were obtained for each tube diameter. The stationary slug lengths were set at approximately 3.5 , 7.0 and 10.0 cm. The glass tube was then inverted, the slug began to rise and the time for its travel to the top of the tube was measured by a stop watch. The tube was then inverted several more times, and the slug travelling time was measured. The rising velocity of slug was calculated by dividing the length of the tube excluding the inserted stopper length and static slug length, by the average slug travelling time.

In the case of carbon tetrachloride which had a density higher than water, the saturated organic liquid poured first into the glass tube and then it was filled up with water. The slug was falling through the aqueous solution instead of rising.

While the slug was rising or falling, the elongated length was roughly measured by a ruler and the stability condition was noted.

2.2. Slug held stationary by downflow of water, with mass transfer

The purpose was to measure the rate of mass transfer of the partially soluble organic component from the slug into a downflow of distilled water. Reverse transfer of water to the organic phase was prevented by having the slug initially water-saturated. This technique of binary mass transfer was first used by Colburn and Welsh[10]. It has the advantage that the mass transfer resistance is confined to one phase, in this case the aqueous phase.

The apparatus used in the mass transfer studies is illustrated in figure 2. The apparatus was mainly made up by three parts; the first part was the connection from the water reservoir to the tube, the second part was the connection of the tube to the aspirator which was fixed to a water tap for suction, the last part was the glass tube itself with three openings. The length of the tube was about 60 cm. Two different internal tube diameters of 4.08 and 6.04 mm were employed in the experiment. The 4.08 mm diameter tube was used for 1-butanol and 1-pentanol (n-amyl alcohol) mass transfer operation, 6.04 mm diameter tube was used only for methyl iso-butyl ketone mass transfer operation. Altogether there were thus three liquid-liquid mass transfer systems.

The opening at the base of the tube as desired to be approximately 4 mm internal diameter, i.e. 6 mm external

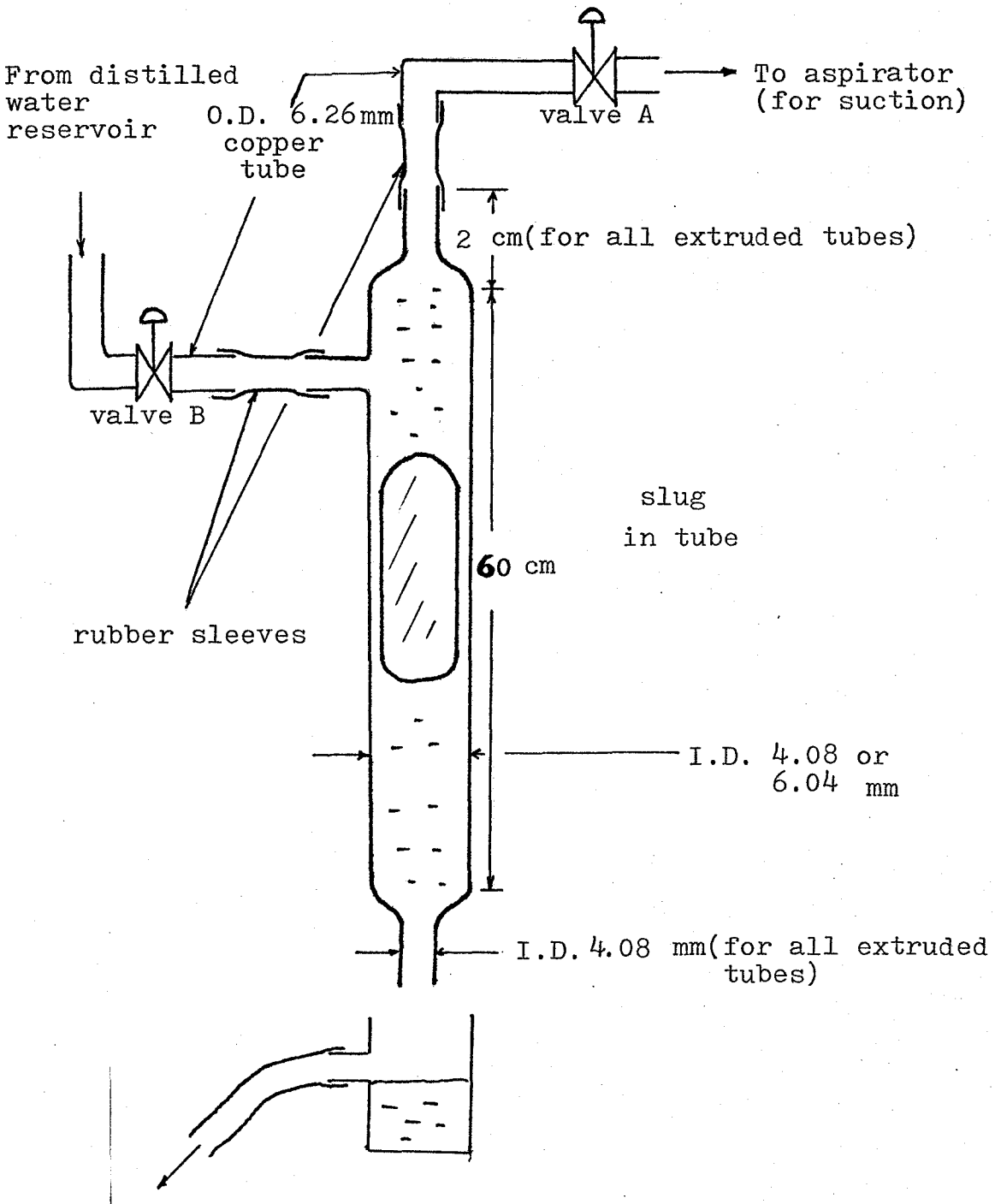

Figure 2. Mass transfer apparatus(not to scale)

diameter, the reason being that 4 mm internal diameter was less than the critical diameter for air in water, so that water could not drain out from the bottom opening of the tube when the two valves were closed, but a steady state flow could be maintained during the mass transfer operation.

In methyl iso-butyl ketone mass transfer operation, 6.04 mm internal tube diameter was used. The top and bottom ends were reduced to 4 mm internal diameter tubes with length of 2 cm; this was not necessary for the other tube since its internal tube diameter was 4.08 mm. For both tubes, the extruded length of the side tube opening was about 2 cm.

Copper tubing(6.26 mm O.D.) was used in the main water supply line and rubber tubes were used to join the glass tube openings to the copper tubing. Two brass needle valves were employed in the system; valve A was used to adjust the amount of suction(initially required to clear the tube), valve B was used to control the flow rate of water going into the glass tube. The reservoir was a cylindrical glass tank with capacity of 20 litres of distilled water. The bottom of the reservoir was 40 cm higher than the side opening of the tube, and this head was sufficient for the maximum flow rate necessary to keep the slug stationary.

A 250 mL beaker was used as a receiver. About 2 cm below the rim of the beaker, an extruded opening about 2 cm

in length and 4 mm internal diameter was made. A long rubber was used to join the side opening to the drain which was about 50 cm below the beaker.

The glass tube was first cleaned with chromic acid and washed with distilled water. Then it was fixed in the required position by a clamp. The aqueous phase in the reservoir was distilled water. Valve B was opened and water was passed down the tube into the receiving beaker. Suction was begun and valve A was carefully adjusted, so that all air was removed from the glass tube. When the tube was totally filled up by distilled water, valve A was closed and then valve B. Water was kept inside the tube, because the opening at the base(4.08 mm I.D.) was below the critical diameter.

The organic liquid, saturated with water, was pipetted from the separation flask to a 100 mL beaker. The beaker was put under the bottom opening and raised up until the 4.08 mm tube was immersed in the organic liquid. Valve A was turned on and a slug of organic phase was sucked into the glass tube. The valve was turned off and the beaker was replaced by the 250 mL receiving beaker. Valve B was turned on and was adjusted so that the slug was held stationary at the lower part of the glass tube. The 250 mL receiving beaker was replaced by a 250 mL empty flask which was weighed, and at the same moment the stop watch was started to time. Then the slug length was measured periodically by a transparent

ruler and the time of each measurement was also recorded. The time interval between each slug length measurement was ranged from 1 minute to 5 minutes. When the shrinkage rate of the slug due to mass transfer was slow, the time interval for the consecutive slug length measurements was about five minutes or less. When the shrinkage rate of the slug was high, a one minute time interval was employed. The slug length measurements were stopped when the slug had shrunk to a non-cylindrical shape; at that point, the slug began to rise from its stationary position, unless the water flow was increased.

The 250 mL flask which had been used to collect the solution dripping down from the tube was removed after a duration of three minutes, and it was immediately replaced by another weighed 250 mL empty flask. After three minutes, the flask was again replaced by another weighed 250 mL empty flask. The procedure was repeated a third time, when the last flask was removed from the tube, nine minutes had elapsed. The weigh-flask was immediately replaced by the receiving beaker. All three flasks with liquid in it were weighed again. The difference in weight in each flask gave the amount of aqueous solution dripped for a period of three minutes. Since the density of the exit solution was approximately same as water, the volumetric flow rate could be calculated. The average of the three volumetric flow rates was taken as

the flow rate for the run.

For each liquid-liquid system, three different initial lengths of slug were studied. The initial lengths of slug ranged from 3 cm to 8 cm. Slug lengths longer than 8 cm would give ripples at the end of the slug.

2.3. Tapered tubes for measurement of critical diameter

A typical glass tapered tube was shown in figure 3. Four different sizes of tapered tube were used in estimating the critical diameter of the organic liquids in water. Since the tubes could not be made cheaply with a precise taper, it was necessary to calibrate the tubes before use. The calibrations were done in the following way. A burette was first filled up with water, the thin end of the tapered tube was then immersed in the water held by the burette and the larger end of the tapered tube was fixed to a pipette filler; water was sucked into the tapered tube which was than raised above the water level in the burette. The height of the water in the tapered tube and the difference in volume of water in the burette were measured. The procedure was repeated for different heights of water level in the tapered tube.

For the larger tapered tubes (tubes III and IV), the calibration procedure was a little bit different. The smaller end of the tube was sealed by a stopper and the length of inserted portion of the stopper was measured. A burette filled with water was used to drip the water into the water into the tapered tube. The height of the water level in the tapered tube and the difference in volume in the burette were measured. Readings were taken as the height of the water level in the tapered tube was increased.

Kerosene, benzene, 1-butanol and carbon tetrachloride

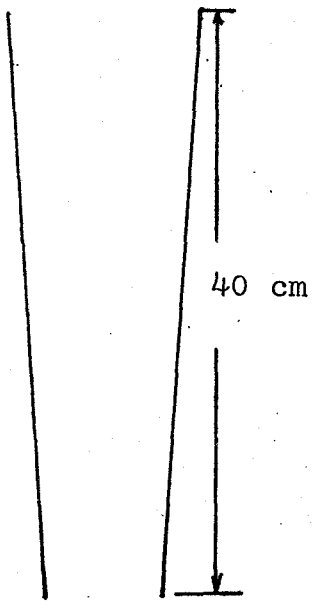

Figure 3. Tapered tube (the diameter did not increase exactly linearly with length)

were the four organic liquids used in the measurement, all of them were saturated with water. For small tapered tubes, the smaller end of the tapered tube was sealed by a finger. The tube was filled with mutually saturated water, organic liquid was then added to the water until it overflowed. The larger end of the tube was sealed by a stopper, then the tube was inverted. The slug rose and finally stopped. The time taken for the slug to become stationary was up to several minutes. The position of the stationary slug was measured by a ruler, and the internal tube diameter was estimated from the calibration of the tapered tube. For the large tapered tube, the smaller end of the tapered tube was sealed by a stopper instead of a finger.

Since carbon tetrachloride had a density higher than water, when the organic liquid was added to the water in the tapered tube, the slug moved down the tapered tube, therefore, inversion of the tube was not necessary.

Six pure liquids in contact with air were also measured in the tapered tubes. They were: water, acetone, 1-butanol, benzene, carbon tetrachloride and ethylene glycol.

The method of relating the internal diameter of the tapered tube to its height was illustrated below:

$$\pi R^2 dh = dV' \qquad (1)$$

$$\pi R^2 = dV/dh \quad (2)$$

$$d = 2R = 2(dV/(\pi dh))^{\frac{1}{2}} \quad (3)$$

Where h was the height from the smaller end of the tapered tube. The calibration and diameter-height relation charts were shown in figures 4 to 10.

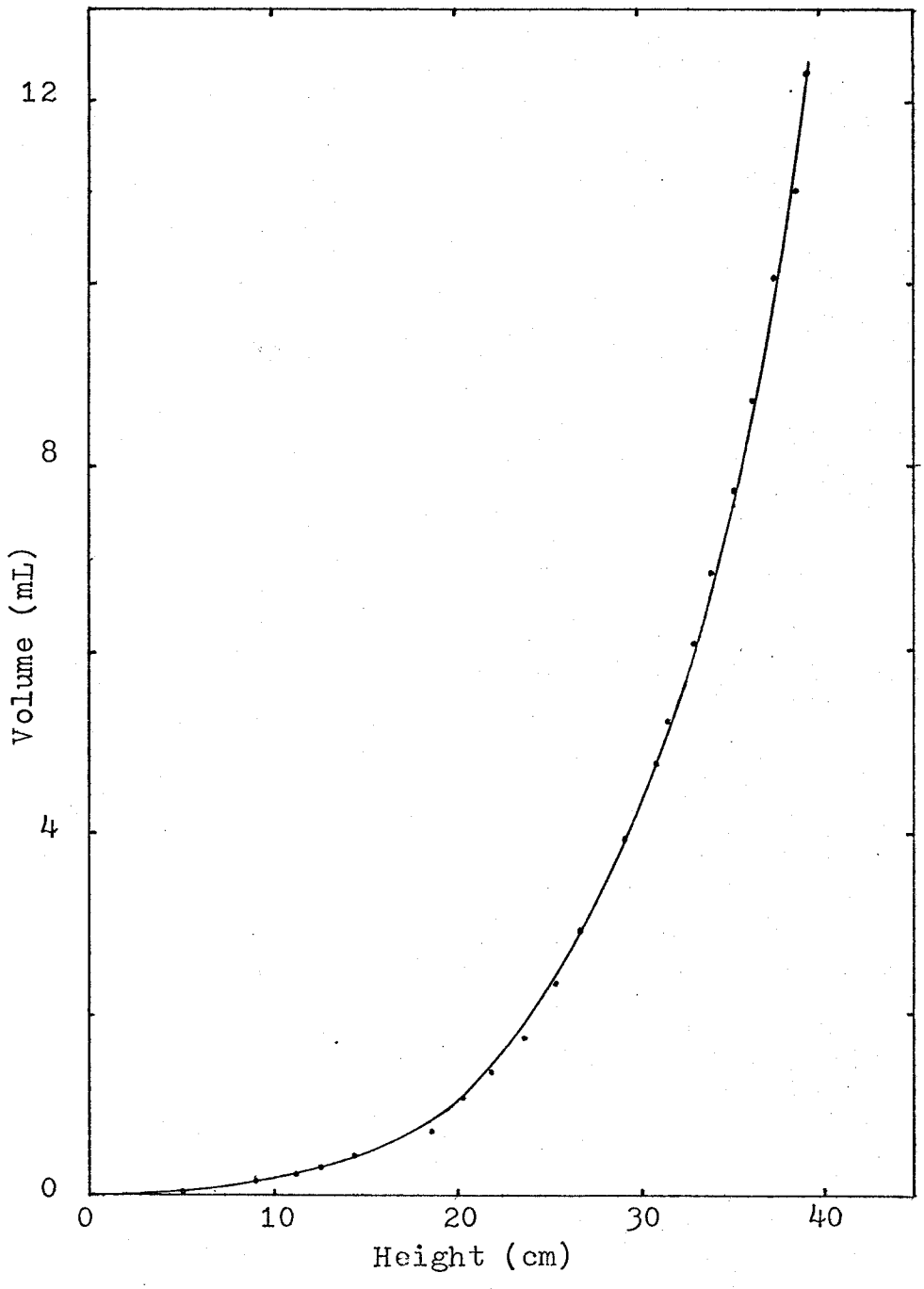

Figure 4. Tapered tube I calibration

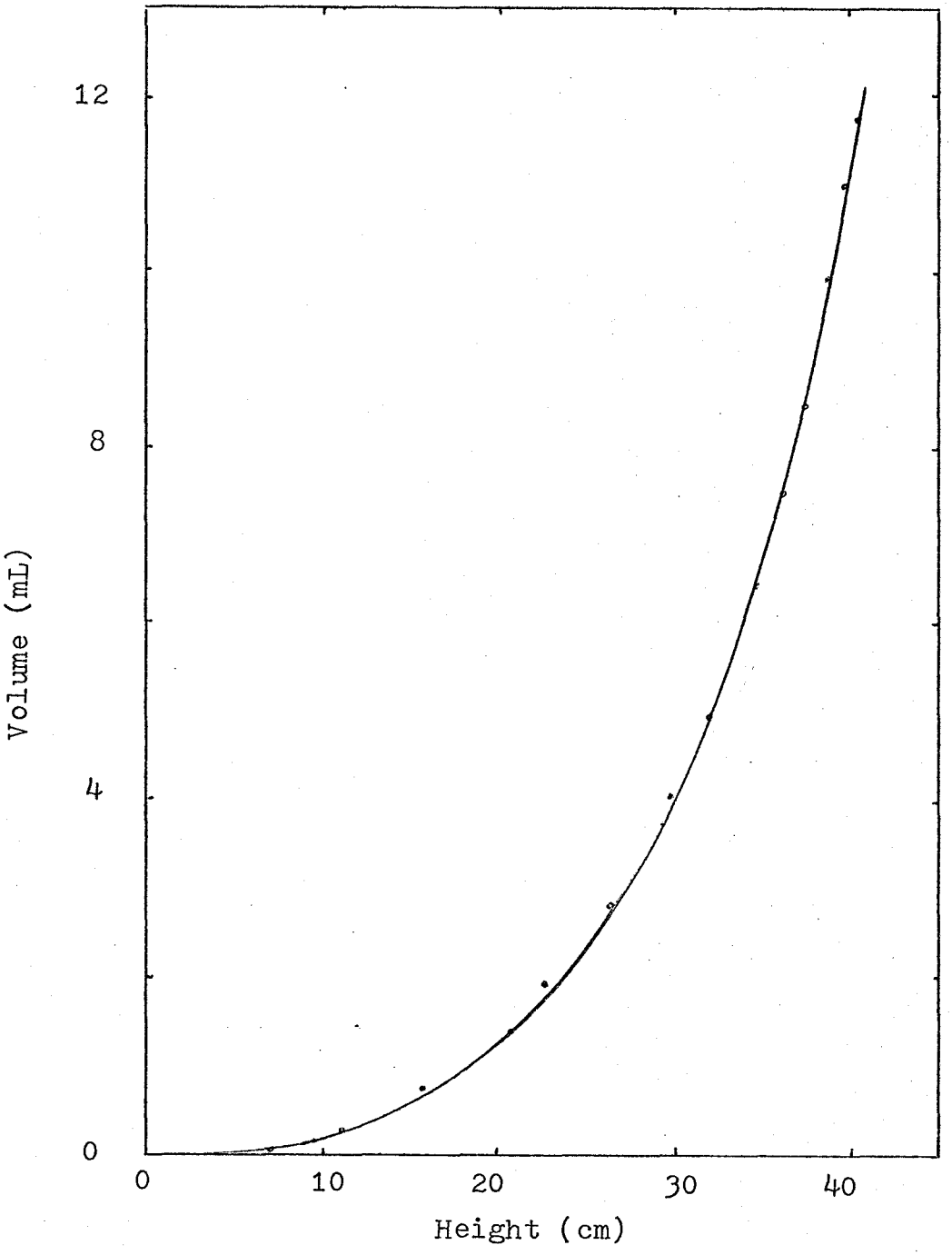

Figure 5. Tapered tube II calibration

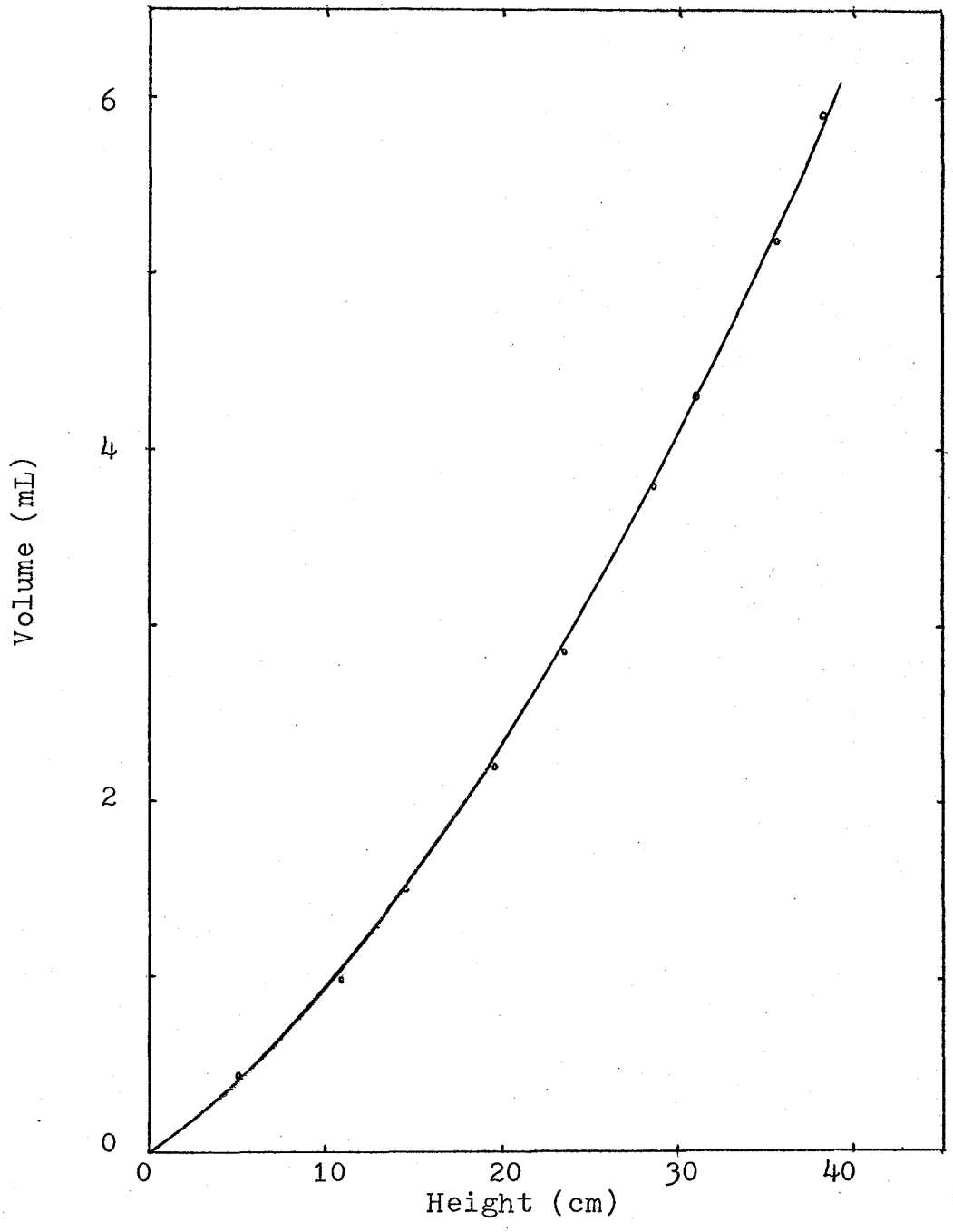

Figure 6. Tapered tube III calibration

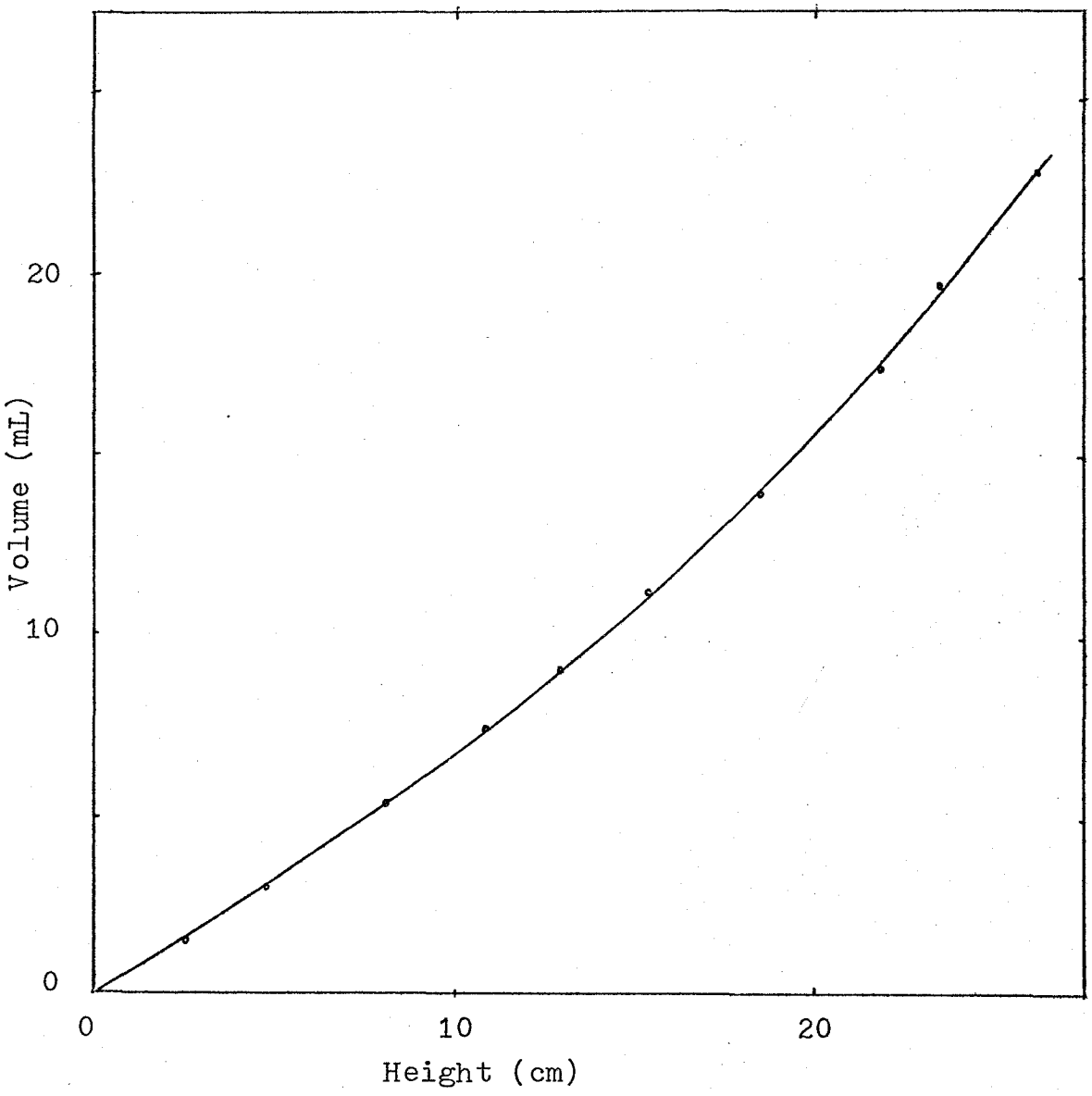

Figure 7. Tapered tube IV calibration

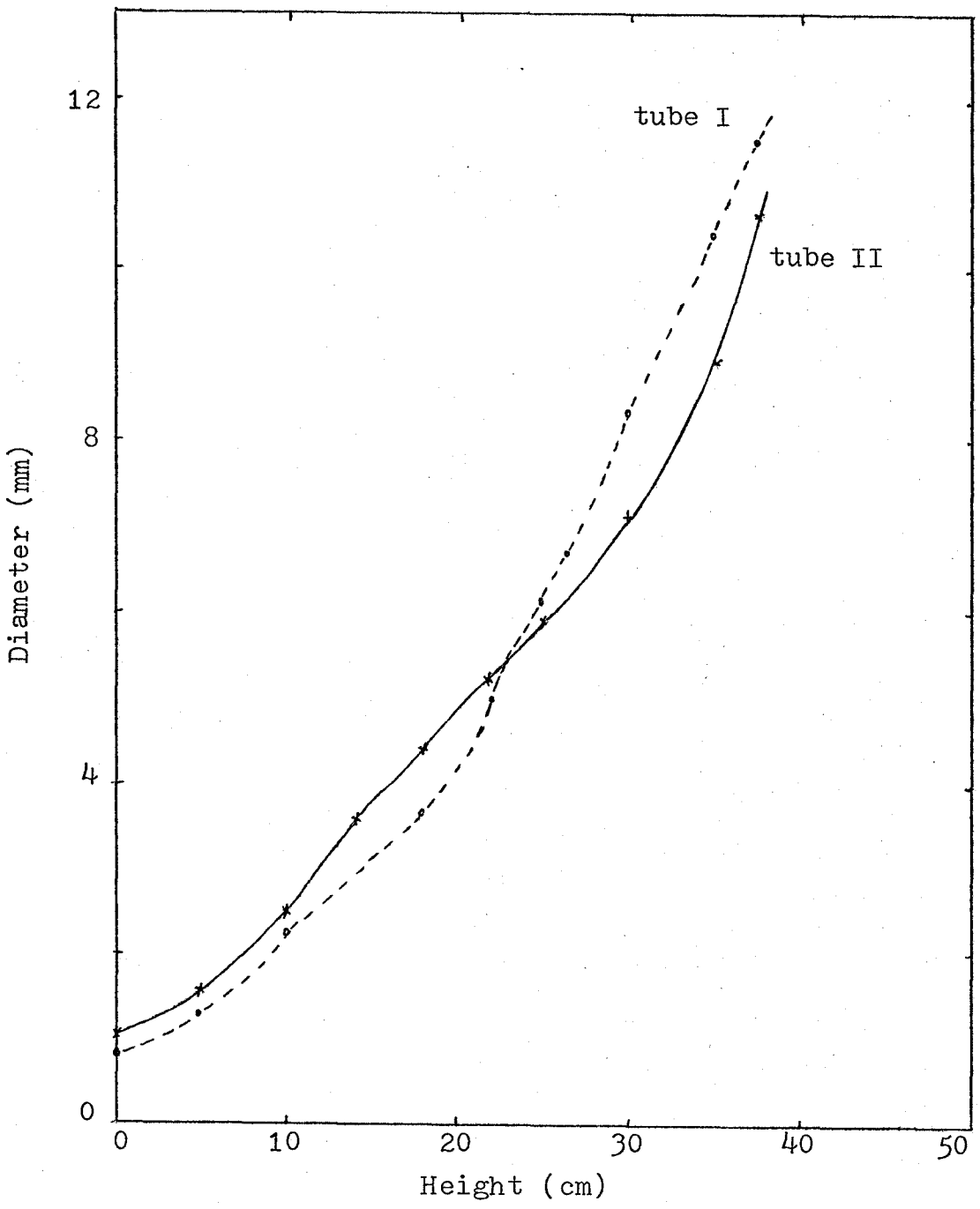

Figure 8. Diameter versus height
(tapered tubes I and II)

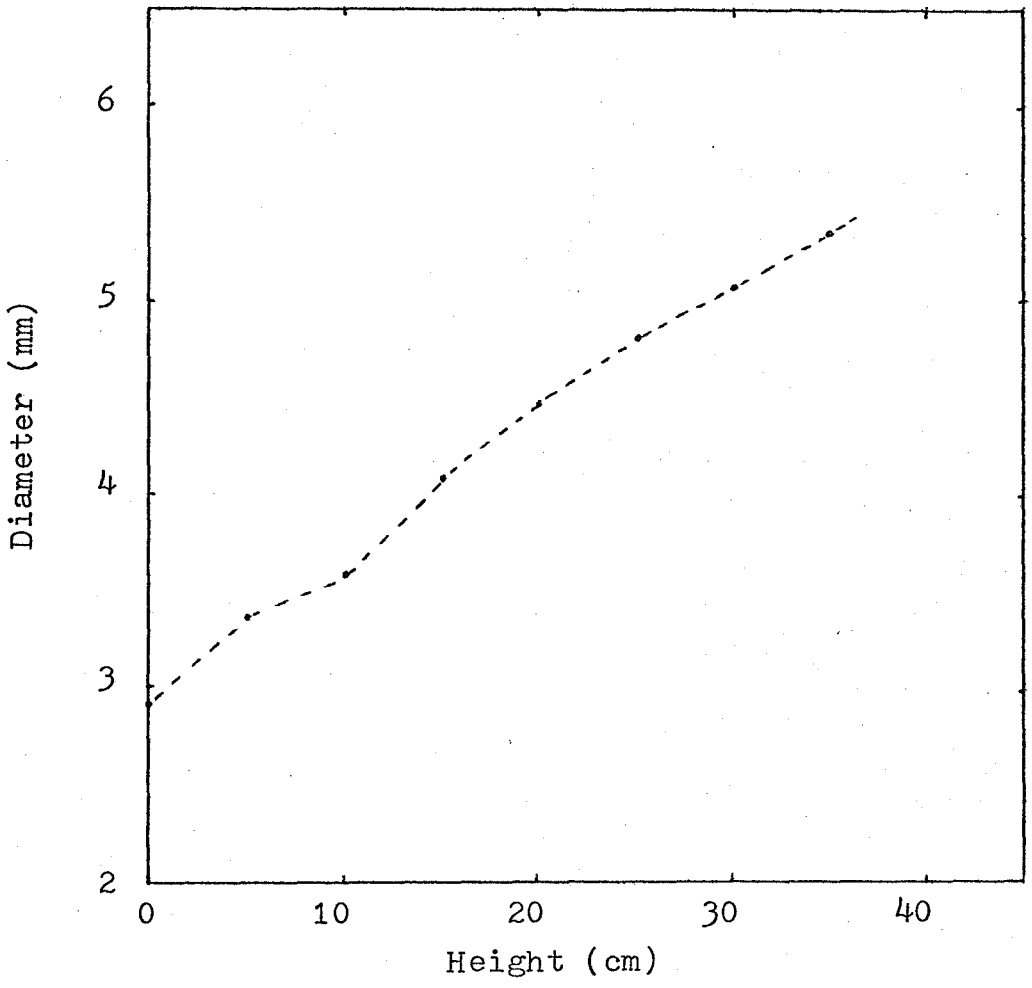

Figure 9. Diameter versus height (tapered tube III)

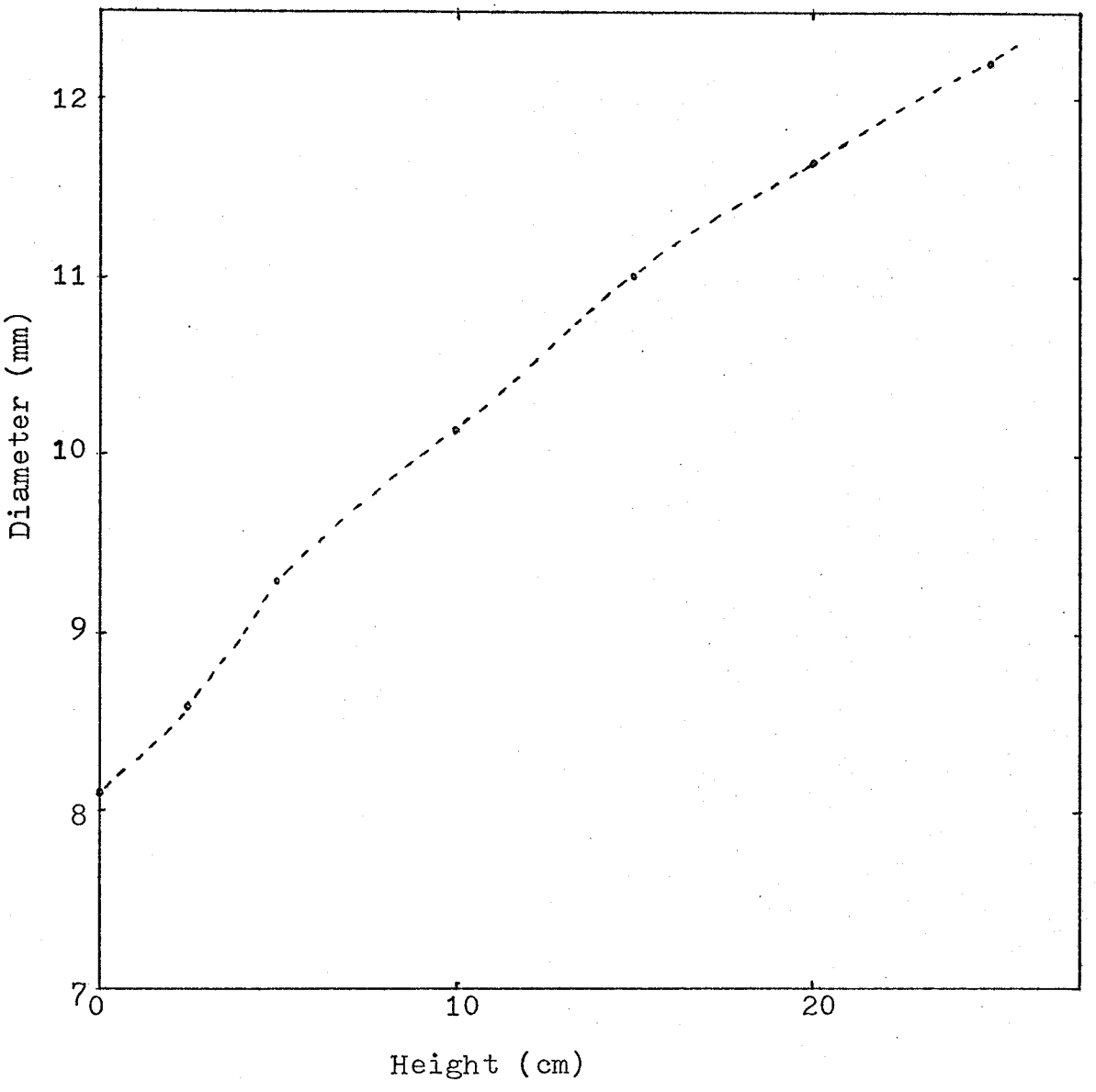

Figure 10. Diameter versus height (tapered tube IV)

2.4. Solubility measurement

A 50 mL burette was used in the solubility measurement. The burette was first filled with distilled water up to more than 25 mL, the volume of distilled water was recorded. Then pure organic liquid was added to the water in a volume less than that of the water, the volume of the pure organic liquid was measured by taking the difference of volume reading in the burette immediately after addition of organic component. The top opening of the burette was stoppered, and the tube was inverted many times so that both phases became mutually saturated. The remaining organic phase volume at equilibrium was measured. Several different initial organic to water volume ratios were performed with the ratio less than one. The organic phase volume at equilibrium was plotted versus initial organic phase volume as shown in figures 11 to 15, the solubility of pure organic liquid in water was found by the intercept of the straight line for zero remaining organic phase volume at equilibrium.

The solubility of water in the organic phase was measured by the same procedure except the aqueous and organic phases were exchanged in the experiment.

3. PROPERTIES OF ORGANIC LIQUIDS USED

All the properties of organic liquids are given at 25°C ± 1°C. Unless the properties are referenced, the data was obtained in this work.

3.1. Viscosity*

Table 1

Organic liquid saturated with water	g/cm.s (poise)	μPa.s
Kerosene	0.0167	1670
Benzene	0.0062	620
Carbon Tetrachloride	0.0091	910
1-Butanol (n-Butyl alcohol)	0.0286	2860
1-Pentanol (n-Amyl alcohol)	0.0352	3520
Methyl iso-Butyl Ketone (MIBK)	0.0057	570

* Viscosity was measured by viscometer.

3.2. Density*

Table 2

Organic liquid - pure	g/mL
Benzene	0.88 [11]
Carbon Tetrachoride	1.595 [11]
1-Butanol (n-Butyl alcohol)	0.81 [11]
1-Pentanol (n-Amyl alcohol)	0.8144 [11]
Methyl iso-Butyl Ketone (MIBK)	0.795

Table 3

Organic liquid saturated with water	g/mL
Kerosene	0.79
Benzene	0.87
Carbon Tetrachoride	1.57
1-Butanol (n-Butyl alcohol)	0.84
1-Pentanol (n-Amyl alcohol)	0.83
Methyl iso-Butyl Ketone (MIBK)	0.81

*Mass divided by volume gave the density. Both mass and volume were measured.

3.3. Solubility

3.3A. Solubility of organic liquid in water*

Table 4

Organic liquid	g organic liquid per 100 mL water
Kerosene	----
Benzene	0.082 [11]
Carbon Tetrachloride	0.08 [11]
1-Butanol (n-Butyl alcohol)	7.86
1-Pentanol (n-Amyl alcohol)	2.69
Methyl iso-Butyl Ketone (MIBK)	2.07

*Solubilities of organic liquids in water were found by the intercepts at the horizontal axes of figures 11 to 13. The method was mentioned in section 2.4.

3.3B. Solubility of water in organic liquid*

Table 5

Organic liquid	g water per 100 mL organic liquid
1-Butanol (n-Butyl alcohol)	19.5
1-Pentanol (n-Amyl alcohol)	9.5
Methyl iso-Butyl Ketone (MIBK)	1.6

*Solubilities of water in organic liquids were found by the intercepts at the horizontal axes of figures 14 to 16. The method was mentioned in section 2.4.

3.3C. Pure organic liquid in wetted organic liquid*

Table 6

Organic liquid	g pure organic liquid per mL wetted oragnic liquid
1-Butanol (n-Butyl alcohol)	0.68
1-Pentanol (n-Amyl alcohol)	0.74
Methyl iso-Butyl Ketone (MIBK)	0.78

*It was calculated from section 3.3B.

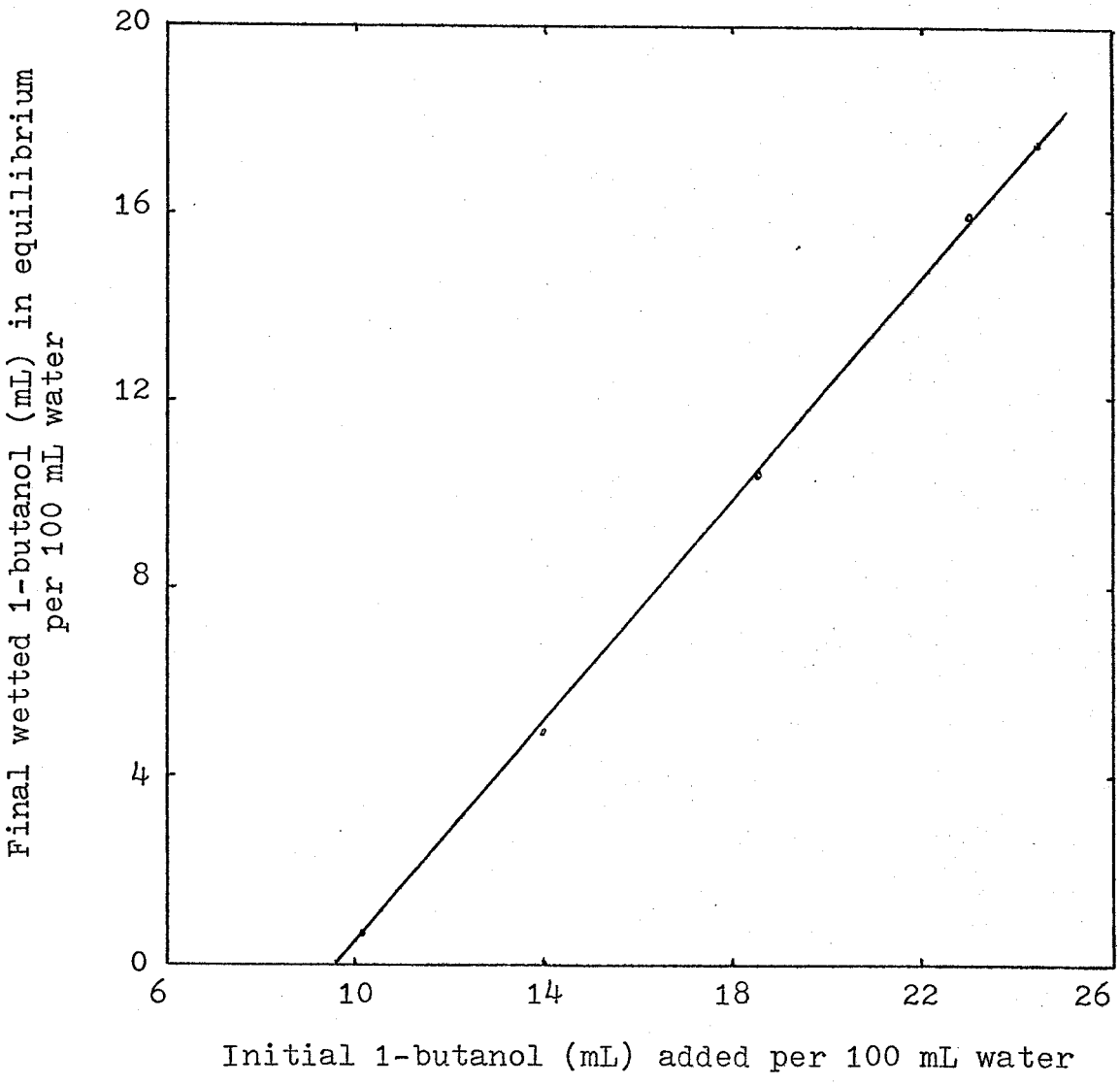

Figure 11. Solubility of 1-butanol in water

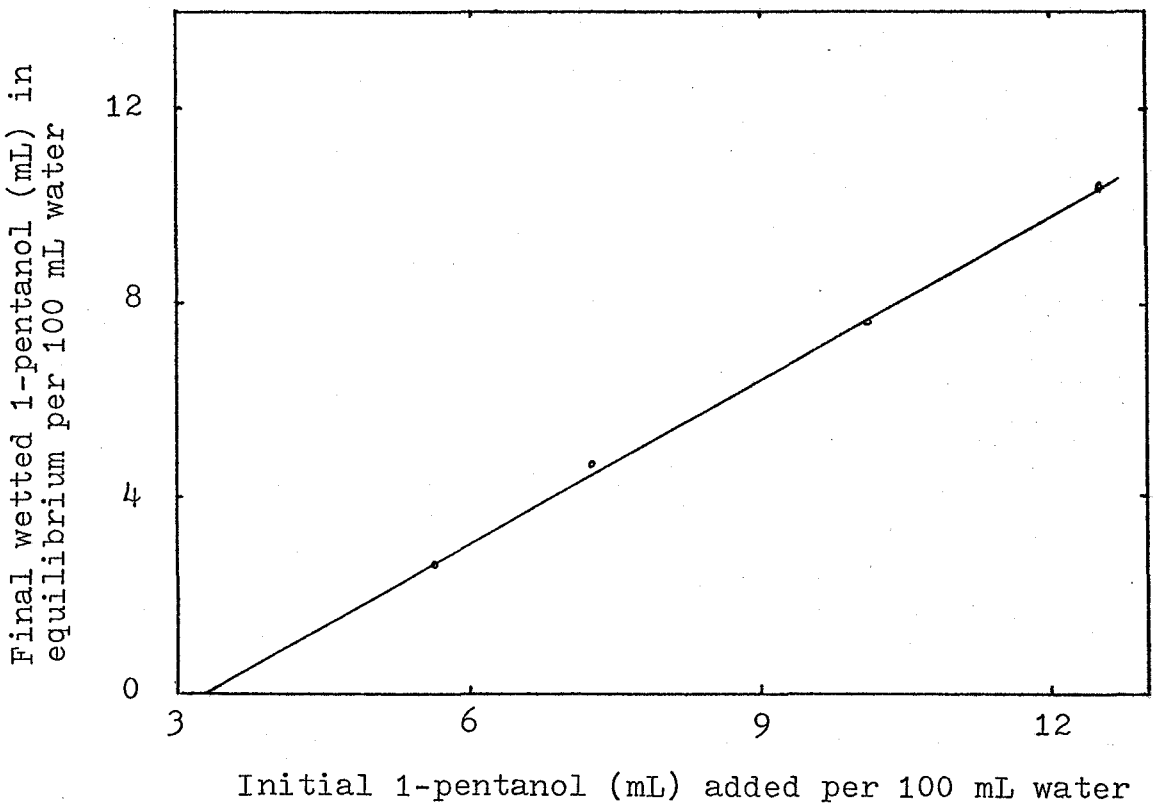

Figure 12. Solubility of 1-pentanol in water

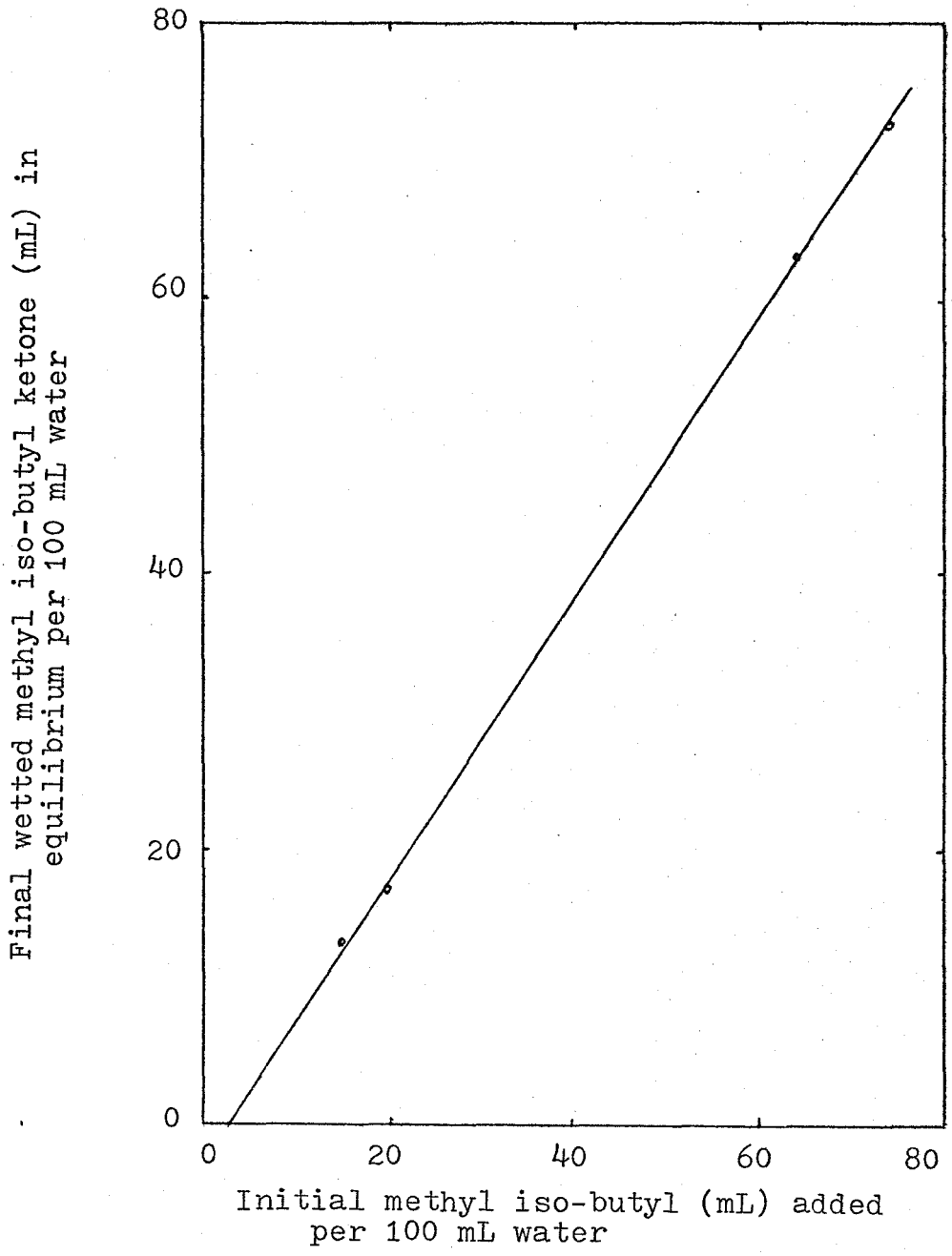

Figure 13. Solubility of methyl iso-butyl ketone in water

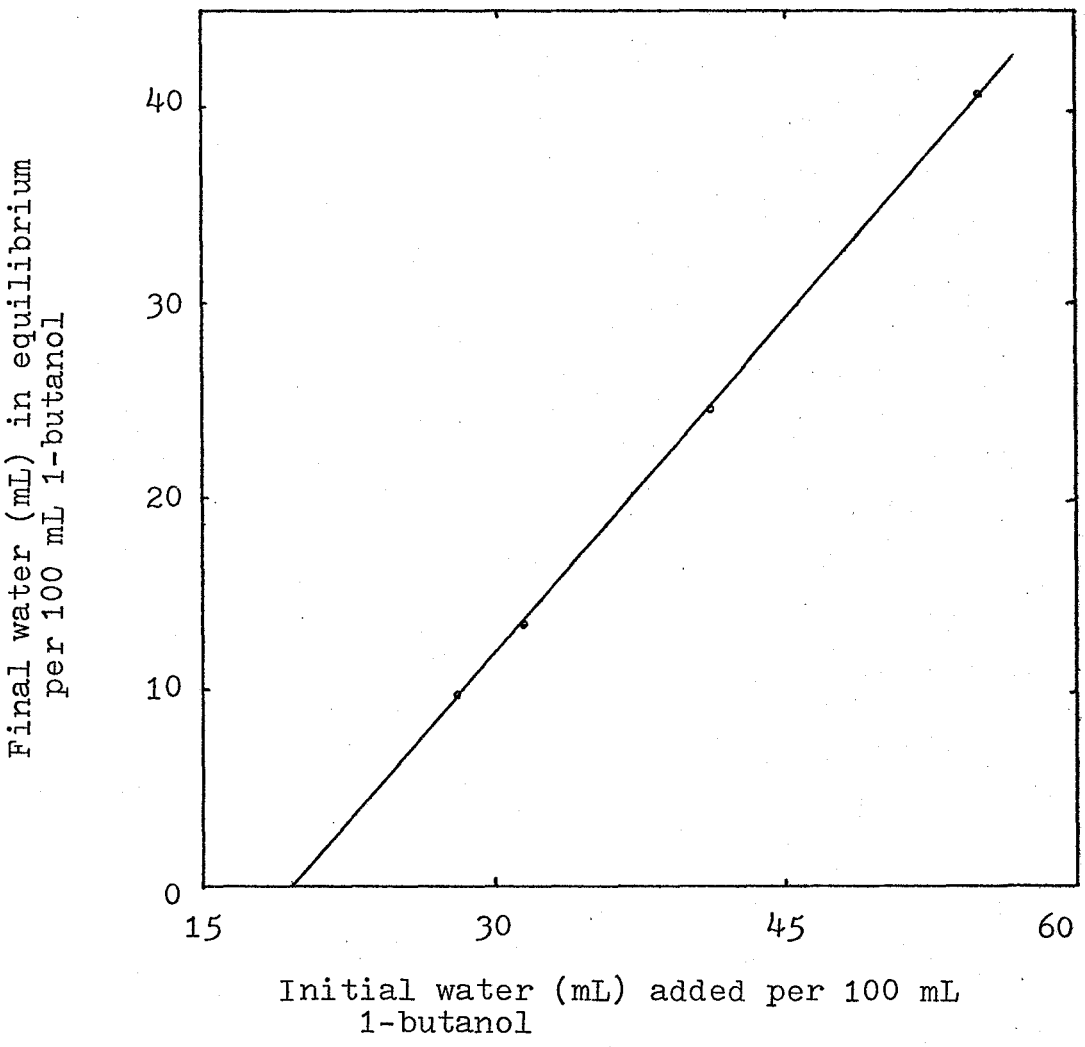

Figure 14. Solubility of water in 1-butanol

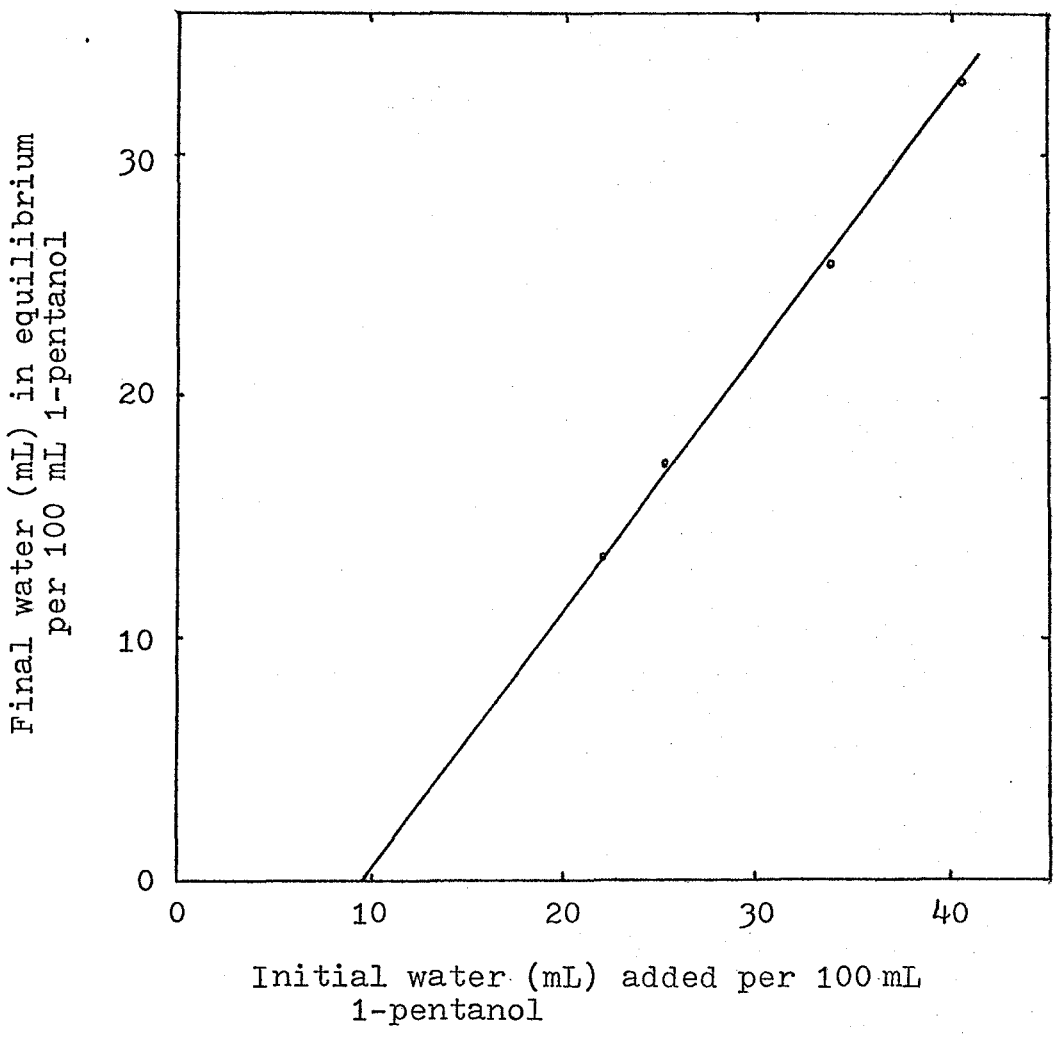

Figure 15. Solubility of water in 1-pentanol

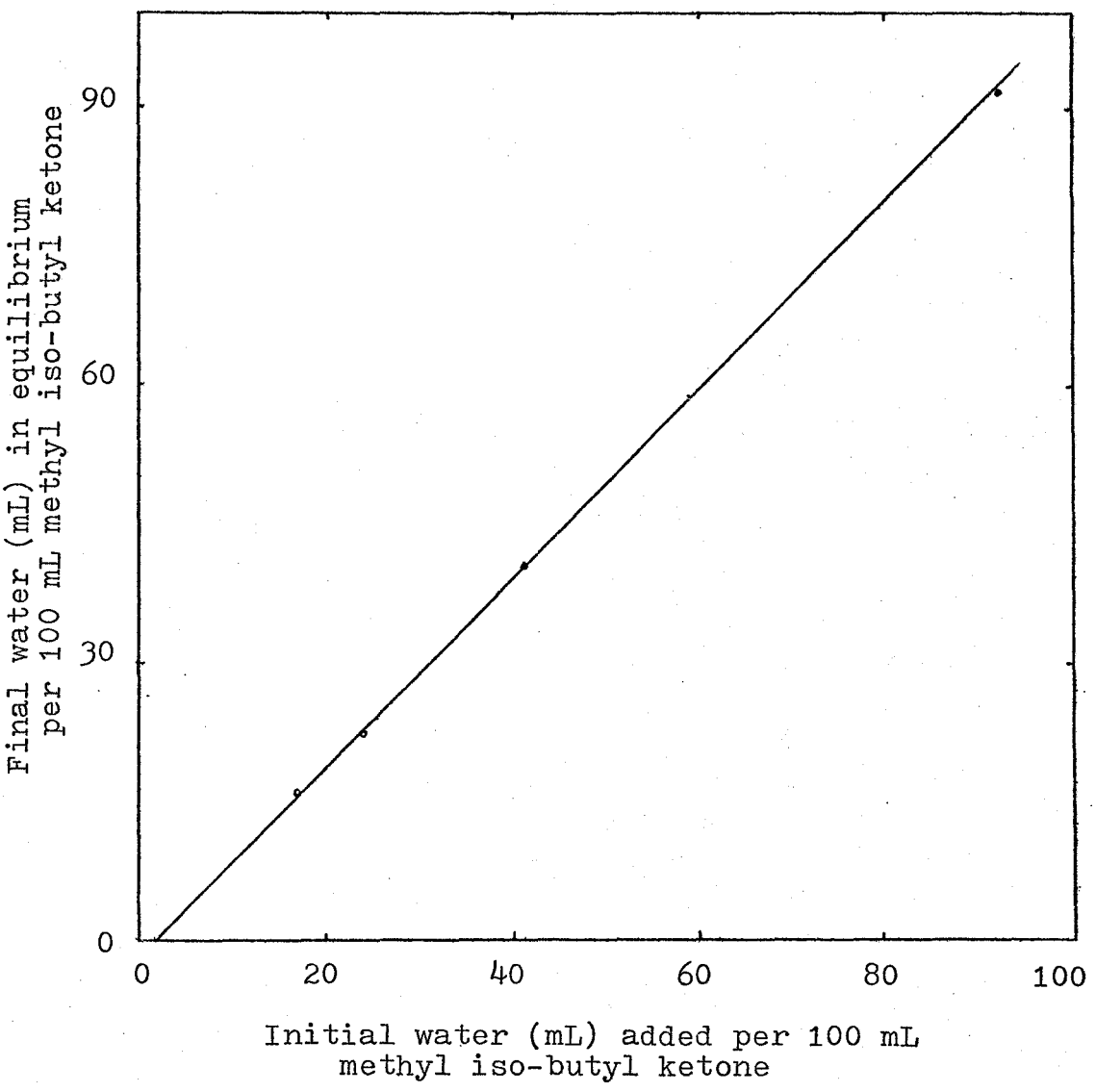

Figure 16. Solubility of water in methyl iso-butyl ketone

3.4. Interfacial tension with respect to water*

Table 7

Organic liquid mutually saturated with water	mN/m
Kerosene	39.3
Benzene	29.1 [12,13]
Carbon Tetrachloride	37.2 [12,13]
1-Butanol (n-Butyl alcohol)	1.8 [13]
1-Pentanol (n-Amyl alcohol)	----
Methyl iso-Butyl Ketone (MIBK)	10.2 [13]

*Interfacial tension was measured by Wilhelmy plate method.

3.5. Diffusivity

Table 8

Organic liquid at infinite dilution in water	$(cm^2/s) \times 10^5$
1-Butanol (n-Butyl alcohol)	0.96 [14]
1-Pentanol (n-Amyl alcohol)	0.826**
Methyl iso-Butyl Ketone (MIBK)	0.77**

**Diffusivity was estimated by the empirical correlation of Wilke and Chang [15].

Table 9

Organic liquid at saturation in water	$(cm^2/s) \times 10^5$
1-Butanol (n-Butyl alcohol)	0.65#
1-Pentanol (n-Amyl alcohol)	----
Methyl iso-Butyl Ketone (MIBK)	----

#Diffusivity at saturation was found by extrapolating the data given by Johnson and Babb [16]; the curve is shown in figure 17.

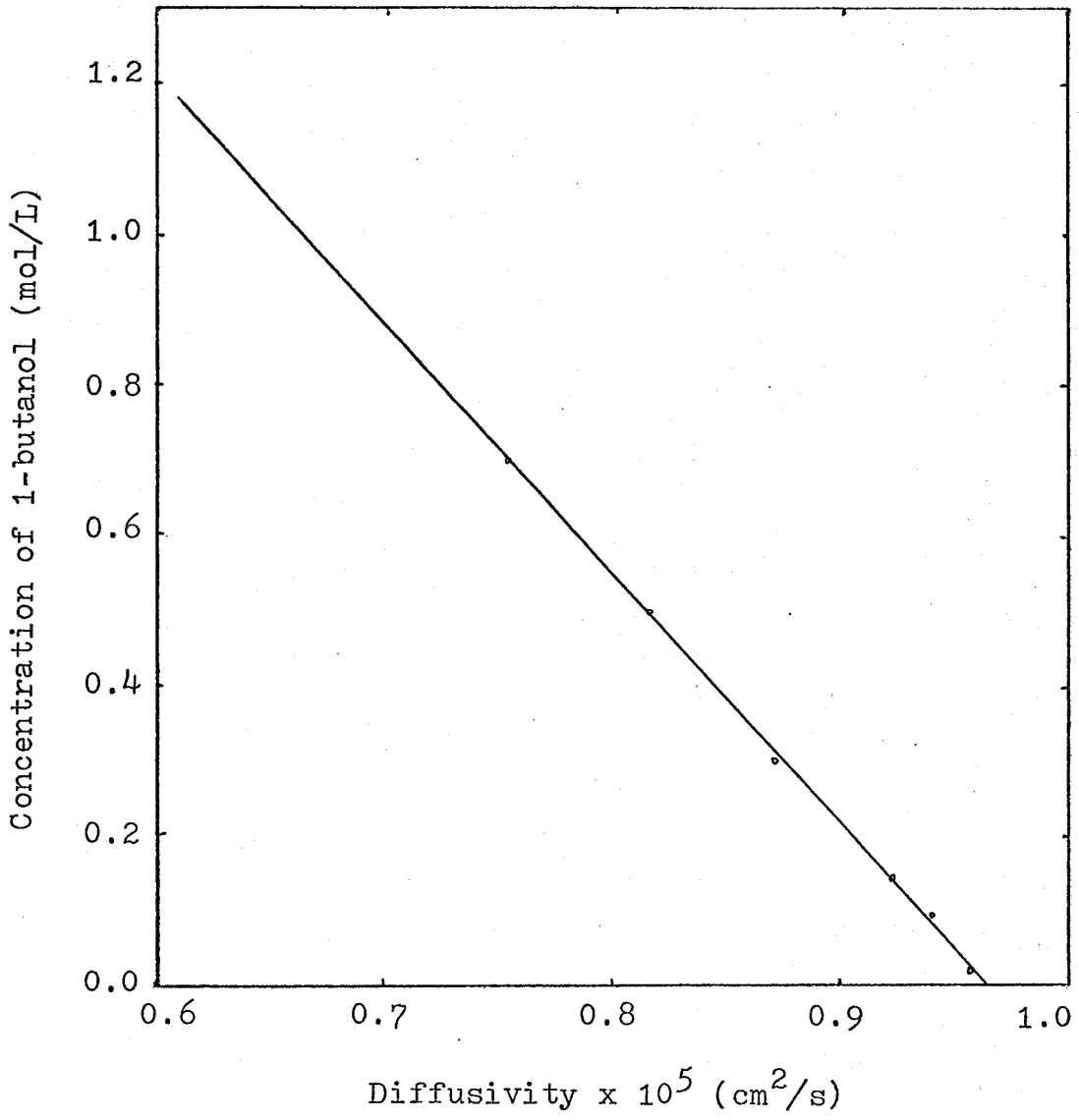

Figure 17. Diffusivity of 1-butanol in water (Johnson and Babb [16])

4. VELOCITIES OF RISING SLUGS IN CLOSED TUBES

4.1. Flow regimes for slugs in gas-liquid systems (Wallis[17])

The velocity V_s of a cylindrical gas bubble rising through a denser liquid is governed by the interaction between buoyancy and other forces. If the viscosity of the gas in the bubble is negligible, the only three forces which are important are those from liquid inertia, liquid viscosity and surface tension. Three dimensionless groups are formed when they are balanced with buoyancy:

$$\frac{\rho_l V_s^2}{D' g(\rho_l - \rho_g)} = k_1^2 \tag{4}$$

$$\frac{\mu_l V_s}{D'^2 g(\rho_l - \rho_g)} = k_2 \tag{5}$$

$$\frac{\sigma}{D'^2 g(\rho_l - \rho_g)} = k_3 \tag{6}$$

Where D' is a characteristic dimension of the duct cross section. When the slug rise is solely determined by the liquid inertia, then

$$V_s = k_1 \rho_l^{-\frac{1}{2}} (gD'(\rho_l - \rho_g))^{\frac{1}{2}} \tag{7}$$

Values of k_1 for cylindrical ducts were obtained by Dumitrescu[18] and by Davies and Taylor[19]. Dumitrescu

found that k_1 was 0.351 which is a little bit higher than the value obtained by Davies and Taylor, they obtained 0.328. Later, White and Beardmore[20] performed a series of experiments and found that the preferred value of k_1 was 0.345.

When viscosity dominates, the equation for slug rise velocity is obtained from the dimensionless group

$$V_s = \frac{k_2 g D'^2 (\rho_l - \rho_g)}{\mu_l} \qquad (8)$$

Wallis[21] found that k_2 was 0.010 which is very close to 0.0096 found by White and Beardmore[20] for vertical round tubes.

When the surface tension dominates, the slug does not move at all. For vertical round tubes, this would occur when

$$N_{EO} = \frac{g D'^2 (\rho_l - \rho_g)}{\sigma} \leq 3.37 \qquad (9)$$

The number 3.37 was obtained by Bretherton[22] and will be discussed later. N_{EO} is called the Eotvos number. When the Eotvos number is equal to 3.37, then the diameter is the minimum possible tube diameter through which a slug of a given system will rise and that diameter is often known as critical diameter.

Since the general solution is governed by three

parameters, it can be presented as a two-dimensional plot of any two chosen dimensionless groups with a third independent dimensionless group as a parameter. k_1 is used to plot against dimensionless inverse viscosity N_f which is obtained by eliminating V_s from first two dimensionless groups. Thus

$$N_f = \frac{(D'^3 g(\rho_l - \rho_g)\rho_l)^{\frac{1}{2}}}{\mu_l} \qquad (10)$$

The third independent parameter is obtained by eliminating V_s and D' from all three dimensionless groups to form the Archimedes number which is given below:

$$N_{Ar} = \frac{\sigma^{3/2}\rho_l}{\mu_l^2 g^{\frac{1}{2}}(\rho_l - \rho_g)^{\frac{1}{2}}} \qquad (11)$$

The experimental data of Wallis is summarised in figure 18, in the form of curves of k_1 versus N_f with N_{Ar} as a parameter.

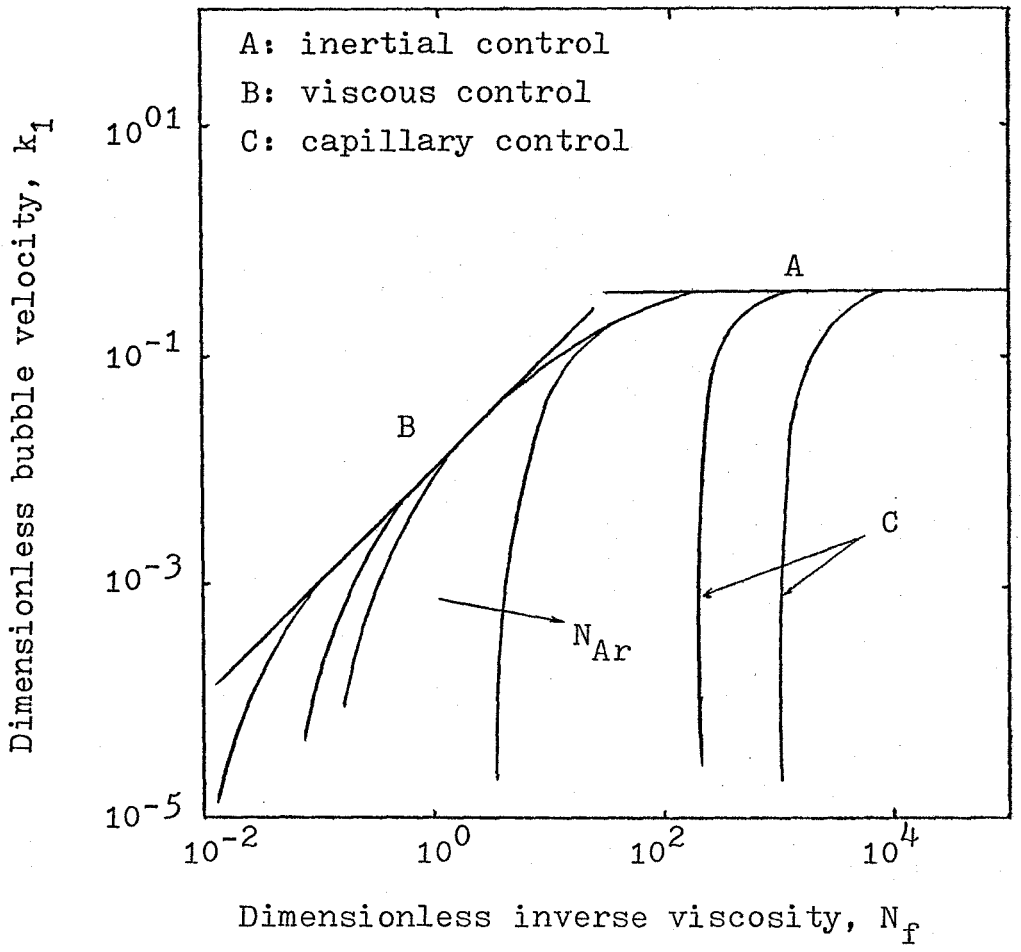

Figure 18. General dimensionless representation of bubble rise velocity in slug flow (Wallis[21])

4.2. Flow regimes for slugs in liquid-liquid systems

Wallis[17] described the slug flow in gas-liquid systems, in which the viscosity of the gas slug is negligible compared to that of the liquid. In liquid-liquid systems, the slug viscosity must also be included in the calculations, and the Wallis plot in figure 18 is just an approximation.

When the slug rise velocity is dominated by the inertia force, equation (4) can be used to describe the slug flow. From the experimental plots of slug velocity versus tube diameter in figure 19, the constant k_1 of equation (4) was found for 1-butanol to be 0.358 which is a little bit higher than the preferred literature value of 0.345. So, 0.358 is used to obtain the inertia dominant regimes. Thus

$$\text{1-Butanol: } V_s = 0.358(0.16gD')^{\frac{1}{2}} \qquad (12)$$

$$\text{Carbon Tetrachloride: } V_s = 0.358(0.57gD')^{\frac{1}{2}} \qquad (13)$$

$$\text{Kerosene: } V_s = 0.358(0.21gD')^{\frac{1}{2}} \qquad (14)$$

$$\text{Benzene: } V_s = 0.345(0.13gD')^{\frac{1}{2}} \qquad (15)$$

All of these four equations were plotted as dotted lines in figure 19. When the surface tension is the dominant force, then equation (9) can be used to find the critical diameter by putting the Eotvos number equal to 3.37. It is found that the critical diameters for 1-butan-

ol, carbon tetrachloride, kerosene and benzene are 1.97 mm, 4.74 mm, 8.02 mm and 8.77 mm respectively. Rough approximations of critical diameter can also be obtained by extrapolating the experimental plot in figure 19, which gives 2.8 mm for 1-butanol, 5.8 mm for carbon tetrachloride, and 11 mm for both kerosene and benzene.

When the tube diameter is slightly larger than the critical diameter, the slug flow is laminar and stable. If the tube diameter is increased further a little bit, then ripples begin to form at the end part of the slug. If the tube diameter is further increased, the slug disperses into droplets.

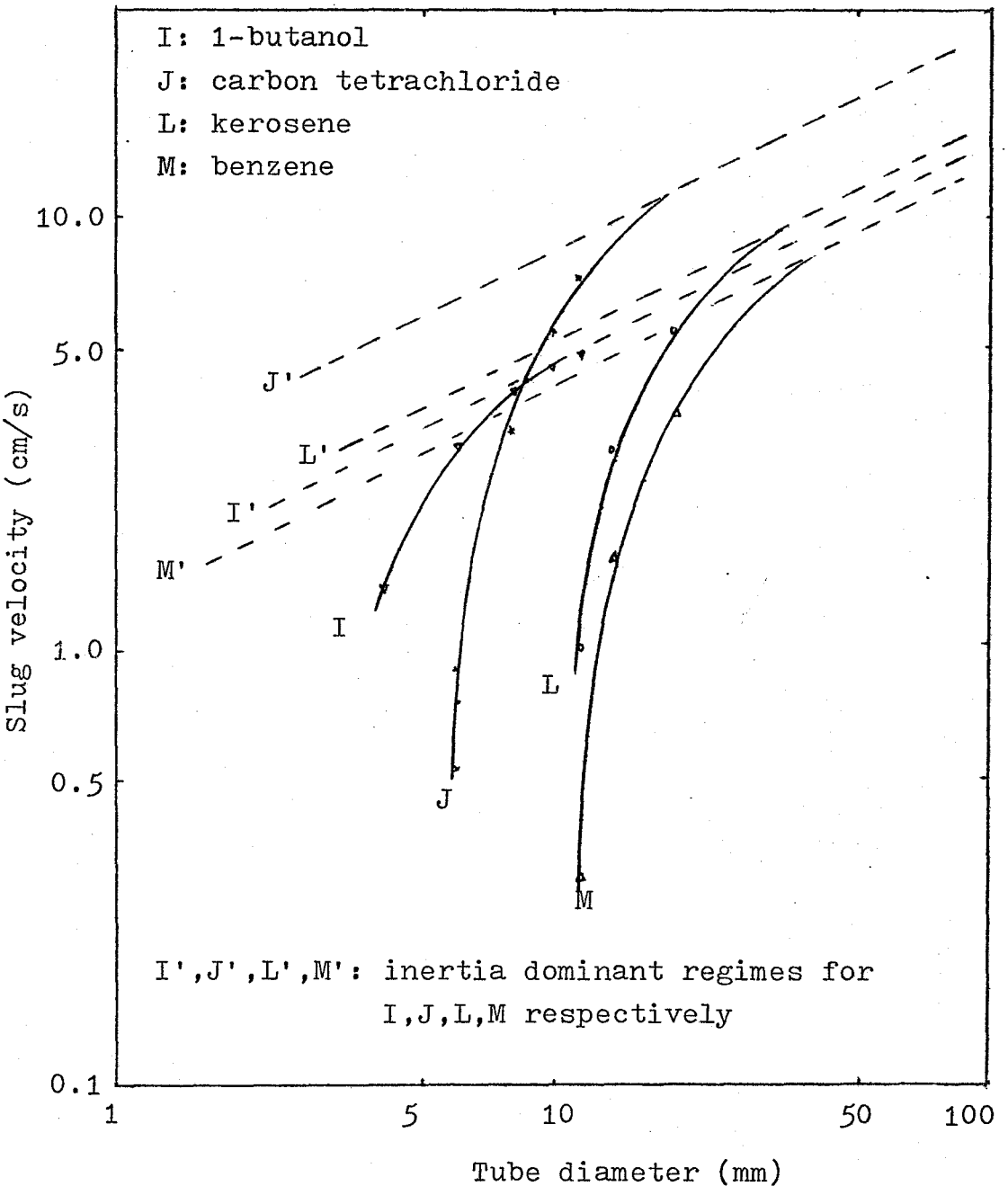

Figure 19. Liquid slug rise velocity versus tube diameter

4.3. Discussion

Since the diameter for zero velocity cannot be obtained by extrapolation from the logarithmic plot, the critical diameter is estimated from the curve at 0.1 cm/s. There is a lack of experimental data at low velocities, so the extrapolation of the curve would not be precise. This is only an approximate method for the critical diameter of a slug flow in liquid-liquid system. The second experimental method is to use the tapered tubes as will be discussed later. The critical diameter calculated by using the Eotvos number of 3.37 is approximately 25% lower than the value obtained by extrapolation method; the difference could be reduced when the tapered tube method is employed.

The best regime for mass transfer operation is the capillary control regime, because it gives a stable laminar slug flow. Therefore, it is preferred to use 4.08 mm diameter tube for 1-butanol, the 6.04 mm diameter tube for carbon tetrachloride, and the 14.69 mm diameter tubes for both kerosene and benzene.

5. CONDITIONS FOR PREVENTION OF SLUG FLOW BY CAPILLARY ACTION

5.1. The motions of long bubbles in tubes (Bretherton[22])

The motion of a long bubble at low Reynolds number in a vertical tube sealed at one end was considered[22]. Observation shows that there is a critical value of $\rho g R^2/\sigma$ below which no rise at all takes place. The bubble rise velocity V_s is low, so that $\mu_1 V_s/\sigma \ll 1$; this implies that the effect of viscous forces on the profile of the bubble will be confined to a region near the tube wall. Axial symmetry was assumed.

From figure 20, the front and rear menisci are separated by region CD, where a uniform film of fluid is draining under the effects of gravity alone. In regions AB, EF the viscous stresses exert a negligible influence on the film profile, which is determined by static equilibrium between surface tension and gravitational stresses.

In regions AB and EF the profile is determined by the condition

$$c_1\sigma = \rho g x \qquad (16)$$

Where c_1 is the mean curvature of the surface and x is the height above some fixed level. Two kinds of profile of region AB are found, which are shown in figure 21. A

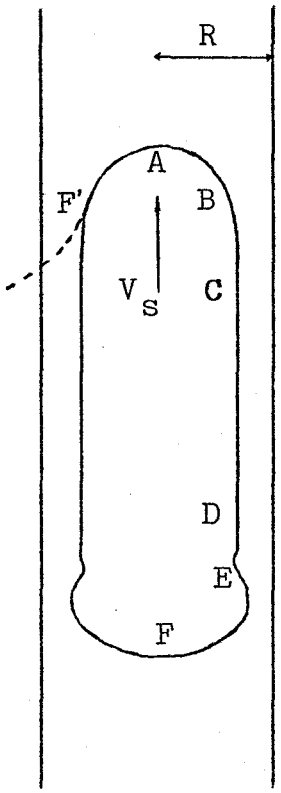

Figure 20. Section of a bubble in a vertical tube (Bretherton[22])

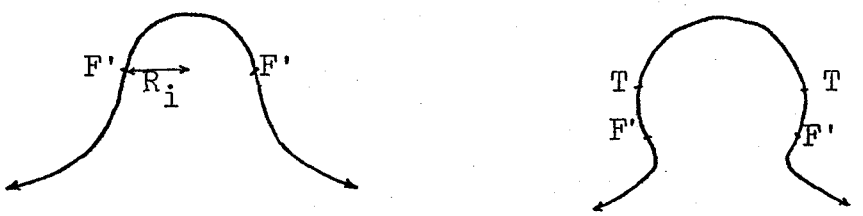

(a) (b)

Figure 21. Equilibrium profiles under surface tension and gravity forces (a) top meniscus $\rho g R_i^2/\sigma > 0.842$ (b) top meniscus $\rho g R_i^2/\sigma < 0.842$ (Bretherton[22])

member of each of these has a point of inflexion F', at which the radius is R_i, but if $\rho g R_i^2/\sigma > 0.842$, as in figure 20(a), there is no point at which the tangent plane is vertical. In figure 20(b), the tangent plane is vertical at a point T. Furthermore, for $|(\rho g R_i^2/\sigma) - 0.842| < 0.2$, the angle θ made with the vertical by the tangent plane at F' is given by

$$\theta = 0.49((\rho g R_i^2/\sigma) - 0.842) \qquad (17)$$

It is expected that for sufficiently small $\mu_1 V_s/\sigma$ the ratio film thickness to tube radius will also be small. The top transition region is shown in figure 22, the equation governing the profile is

$$y_1''' - \frac{g}{\sigma} = \frac{3\mu_1 V_s}{y_1^3 \sigma}\left(y_1 - b - \frac{\rho g b^3}{3\mu_1 V_s}\right) \qquad (18)$$

In addition to equation (18), a continuity of flow is also required. The fluid displaced by the top meniscus of the rising bubble should flow through the uniform region CD to the lower meniscus. Thus

$$-\frac{\rho g b^3}{3\mu_1} = V_b = -\frac{1}{2\pi R}(V_s \pi (R - b)^2) \qquad (19)$$

i.e. $$\frac{\rho g b^2}{3\mu_1 V_s} \doteq \frac{R}{2b} \qquad (20)$$

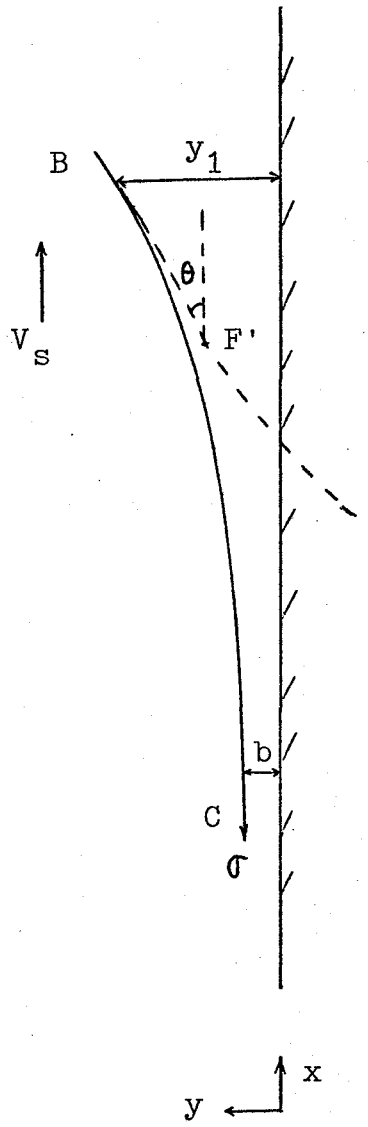

Figure 22. The top transition region

For sufficiently small b/R the last term on the right-land side of equation (18) greatly exceeds the other two throughout region BCDE, and the film profile is given by

$$y_1''' = \frac{\rho g}{\sigma}\left(1 - \frac{b^3}{y_1^3}\right) \tag{21}$$

This may be made dimensionless by the substitution

$$y_1 = b\eta \quad , \quad x = b(\rho g b^2/\sigma)^{-1/3}\xi \tag{22}$$

to give $$\eta''' = \frac{\eta^3 - 1}{\eta^3} \tag{23}$$

In the region CD, $y_1 \doteqdot b$, $\eta''' \doteqdot 3(\eta - 1)$. The equation (22) shows that for sufficiently small $\rho g b^2/\sigma$, provided b/R is also small, there exist regions in which

$$\eta = y_1/b \ll 1 \tag{24}$$

$$y_1/R = b\eta/R \ll 1 \tag{25}$$

$$y_1' = (\rho g b^2/\sigma)^{1/3}\eta \ll 1 \tag{26}$$

Here equation (21) is still valid, but $\eta''' \doteqdot 1$ and

$$\eta = \frac{\xi^3}{6} + \frac{P\xi^2}{2} + Q\xi + R' \tag{27}$$

For a profile of type shown in figure 21(a), provided θ is small or $\rho g R_i^2/\sigma$ is only slightly greater than 0.842. With origin chosen so that P= 0, numerical integration for a top meniscus gives

$$P = 0 \quad , \quad Q = 0.572 \quad , \quad R' = 1.0$$

At the point of inflexion F'

$$y_1 = 1.10b \quad , \quad y_1' = 0.572(\rho g b^2/\sigma)^{1/3}, \quad R_i = R - y_1 \tag{28}$$

Inertion in equations (17),(20) gives

$$\frac{\rho g R^2}{\sigma} - 0.842 = 1.10(b/R)^{2/3} + 1.85b/R$$
$$= 1.25\left(\frac{\mu_1 V_s}{\sigma}\right)^{2/9} + 2.24\left(\frac{\mu_1 V_s}{\sigma}\right)^{1/3} \tag{29}$$

When $V_s = 0$,

$$\frac{\rho g R^2}{\sigma} - 0.842 = 0 \tag{30}$$

or
$$\frac{\rho g d^2}{\sigma} = 3.37 \tag{31}$$

5.2. Tapered tube measurements in gas-liquid and liquid-liquid systems

The temperature for all the measurements was 25°C ± 1°C. Unless the physical properties are referenced, they were measured in this work.

Table 10. Air-liquid contact measurements (tapered tubes I and II)

Liquid	$d_{crit.}$ (mm)			ρ_l^{23} (g/mL)	σ^{23} (mN/m)	N_{EO}
	tube I	tube II	average			
Water	4.6	5.05	4.8	1.0	72	3.14
Acetone	3.25	3.0	3.21	0.787	23.1	3.21
1-Butanol	3.5	3.1	3.3	0.81	24.6	3.51
Benzene	3.16	2.68	2.9	0.876	28.2	2.56
Carbon Tetrachloride	2.2	2.1	2.15	1.59	26.3	2.74
Ethylene Glycol	4.2	3.8	4.0	1.11	48.2	3.61

Table 11. Air-liquid contact measurements (tapered tube III)

Liquid	$d_{crit.}$ (mm)	ρ_l^{23} (g/mL)	σ^{23} (mN/m)	N_{EO}
Water	5.16	1.0	72	3.62
Acetone	3.14	0.787	23.1	3.29
1-Butanol	3.25	0.81	24.6	3.42
Benzene	3.30	0.876	28.2	3.32
Carbon Tetrachloride	----	1.59	26.3	----
Ethylene Glycol	4.00	1.11	48.2	3.61

Table 12. Water-liquid contact measurements* (tapered tubes I and II)

Liquid	$d_{crit.}$(mm)			N_{EO}**
	tube I	tube II	average	
1-Butanol	1.5	2.18	1.8	2.82
Kerosene	8.82	8.5	8.7	3.96
Carbon Tetrachloride	4.4	4.95	4.7	3.32
Benzene	9.7	9.35	9.5	3.95

Table 13. Water-liquid contact measurements* (tapered tube IV)

Liquid	$d_{crit.}$(mm)	N_{EO}**
1-Butanol	----	----
Kerosene	8.32	3.62
Carbon Tetrachloride	----	----
Benzene	9.30	3.78

*Both were mutually saturated. **It was calculated with interfacial tensions from table 7.

5.3. Discussion

Bretherton[22] derived the critical diameter equation only for gas-liquid systems, but it seems that it is also valid in liquid-liquid systems by using interfacial tension instead of surface tension and density difference instead of density. Six liquids were employed for the air-liquid contact using the tapered tubes to test the Eotvos number of 3.37. It is found that the results scatter around 3.37. The average Eotvos number in table 10 is 8% lower than 3.37 and in table 11 is 2% higher than 3.37.

In the liquid-liquid systems, the water and organic liquids were mutually saturated with each other in the tapered tubes. From table 12, it appears that the average Eotvos number is 4% higher than 3.37, while kerosene gives an Eotvos number 18% higher than 3.37. The situation is improved a little bit when a large tapered tube (tube IV) is used, kerosene shows only 7% deviation. The large tapered tube is better than smaller ones because it shows a more gradual decreasing of diameter of the tube. Since none of the four tapered tubes used showed a constant rate of decrease in diameter, the accuracy of the results obtained has been adversely affected. Therefore, it is strongly recommended to use a precisely made tapered tube. Unfortunately such a tube would have to be specially made at great expense.

Three additional factors would influence the measurement of the critical diameter. The first one is the contamination of the liquids, whereby the interfacial tension could be changed. The second one is the contact angle which the slug makes with the tube wall. In a vertical tube with clean solutions, the contact angle is zero; but in a tapered tube with possible contaminants, the contact angle might no longer be zero. The third one is the accuracy of the interfacial tension data. A 0.5 mN/m change in interfacial tension could change the result 30% in the case of 1-butanol mutually saturated with water.

Though there are many possible deficiencies in the critical diameter measurement, yet the results show a reasonable approximation to the Bretherton correlation, and it is felt that better results could be obtained with precision tapered tubes.

6. CALCULATION OF VELOCITY PROFILES IN SLUG FLOW

6.1. Assumptions

The following assumptions are made for the calculation of slug velocity profile:

1. the slug is vertical,
2. there is no radial velocity component,
3. the slug flow is laminar and stable,
4. continuity of shear occurs at the interface,
5. the slug flow is steady,
6. the slug has a cylindrical configuration with axial symmetry,
7. nose and tail effects are neglected, although the overall velocity of the slug is governed by such effects (see figure 19). The relative slug velocity is given from experimental measurement.

6.2. Navier Stokes equations and boundary conditions

A cylindrical slug of the lighter organic dispersed phase with viscosity μ_o and density ρ_o is suspended in the tube. The aqueous continuous phase is contained in a vertical tube, which preferentially wets the tube walls, with viscosity μ_a and ρ_a, flows down relatively to the slug in the annular space. A schematic view of a slug is shown in figure 23.

The flow pattern in each phase is described by the Navier Stokes equations, subject to the assumptions of 6.1.

$$P' - \rho g = \frac{\mu d}{r dr}\left(r\frac{dV}{dr}\right) \qquad (32)$$

Successive integrations give

$$\left(\frac{P' - \rho g}{\mu}\right)\frac{r^2}{2} = r\frac{dV}{dr} + U_1 \qquad (33)$$

$$\left(\frac{P' - \rho g}{\mu}\right)\frac{r^4}{4} = V + U_1 \ln r + U_2 \qquad (34)$$

The values of U_1 and U_2 for each phase are found by employing the boundary conditions.

The organic phase velocity reaches a maximum at the centre of the tube. Thus

when $r = 0$, $\quad \frac{dV_o}{dr} = 0 \qquad (35)$

$$\therefore U_{1o} = 0 \qquad (36)$$

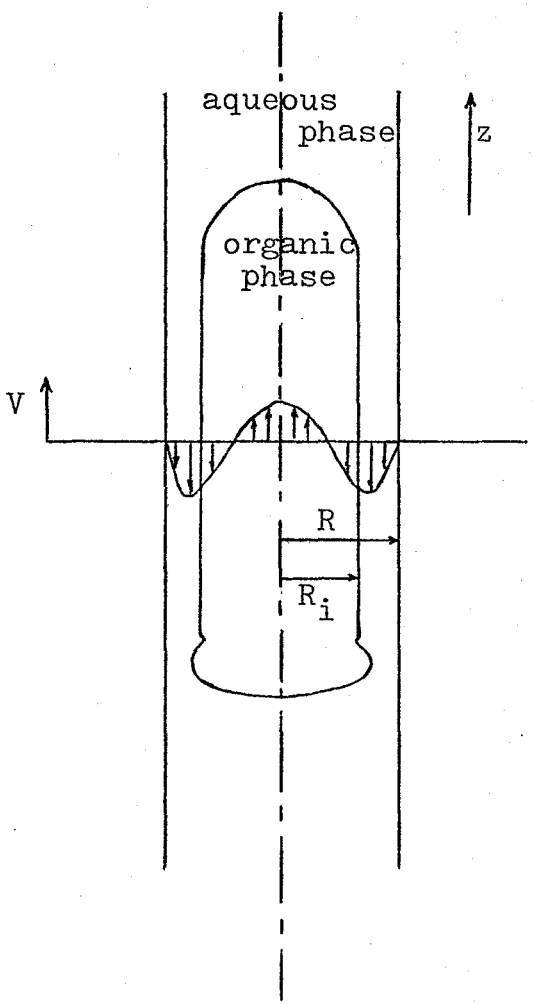

Figure 23. Schematic view of a slug

At the liquid-liquid interface,

$$r = R_i \quad \text{and} \quad V_o = V_a \tag{37}$$

$$U_{2o} = \left(\frac{P' - \rho_o g}{\mu_o}\right)\frac{R_i^2}{4} - V_i \tag{38}$$

The organic phase velocity profile obtained from equations (34), (36) and (38) with condition that $r < R_i$ is

$$V_o = V_i + \left(\frac{P' - \rho_o g}{4\mu_o}\right)(r^2 - R_i^2) \tag{39}$$

In the aqueous phase, two boundary conditions at the interface are employed. The shear stress is equal on either side of the interface. Thus

$$\left(\mu_a \frac{dV_a}{dr}\right)_i = \left(\mu_o \frac{dV_o}{dr}\right)_i = (P' - \rho_o g)R_i/2 \tag{40}$$

$$\left(\frac{dV_a}{dr}\right)_i = (P' - \rho_o g)R_i/(2\mu_a) \tag{41}$$

By substituting equation (41) into equation (33),

$$U_{1a} = \frac{(P' - \rho_a g)R_i^2}{2\mu_a} - \frac{(P' - \rho_o g)R_i^2}{2\mu_a} \tag{42}$$

$$U_{1a} = -\frac{(\rho_a - \rho_o)gR_i^2}{2\mu_a} \tag{43}$$

At the interface,

$$V_a = V_i \quad \text{and} \quad r = R_i \tag{44}$$

$$U_{2a} = \frac{(P' - \rho_a g)R_i^2}{4\mu_a} - V_i + \frac{(\rho_a - \rho_o)gR_i^2 \ln R_i}{2\mu_a} \tag{45}$$

The aqueous phase velocity profile obtained from equations (34), (43) and (45) with condition that $R_i < r < R$ is

$$V_a = \frac{(P' - \rho_a g)(r^2 - R_i^2)}{4\mu_a} + V_i + \frac{(\rho_a - \rho_o)gR_i^2 \ln(r/R_i)}{2\mu_a} \tag{46}$$

The boundary condition at the tube wall allows the interfacial velocity to be calculated.

At $r = R$, $V_a = 0$ (47)

$$V_i = \frac{(P' - \rho_a g)(R_i^2 - R^2)}{4\mu_a} + \frac{(\rho_a - \rho_o)gR_i^2 \ln(R_i/R)}{2\mu_a} \tag{48}$$

By substituting equation (48) into equations (39) and (46),

$$V_o = \frac{(P' - \rho_a g)(R_i^2 - R^2)}{4\mu_a} + \frac{(P' - \rho_o g)(r^2 - R_i^2)}{4\mu_o} + \frac{(\rho_a - \rho_o)gR_i^2 \ln(R_i/R)}{2\mu_a} \tag{49}$$

$$V_a = \frac{(P' - \rho_a g)(r^2 - R^2)}{4\mu_a} + \frac{(\rho_a - \rho_o)gR_i^2 \ln(r/R)}{2\mu_a} \tag{50}$$

These solutions are applicable either to the case where a slug rises in a stagnant dense phase, or to the case where a slug is suspended in a downflow of the continuous phase. The vertical pressure gradient P' is not the same in the two cases and must be calculated from continuity relationships.

6.3. Solution for a slug rising through stagnant liquid

In a given experimental situation, the rising velocity of a slug is measured as V_s. The slug rising velocity depends on the physical properties of the system (in particular, interfacial tension) and is not derived from the first principles. Thus, from continuity considerations,

$$\pi R_i^2 V_s = \int_0^{R_i} 2\pi r V_o dr \qquad (51)$$

The downflow of a aqueous phase must be equal and opposite to the upflow of the organic phase in this case, therefore

$$-\pi R_i^2 V_s = \int_{R_i}^{R} 2\pi r V_a dr \qquad (52)$$

From equations (49) and (51)

$$\pi R_i^2 V_s = 2\pi\left(\left(\frac{P' - \rho_a g}{4\mu_a}\right)\left(\frac{R_i^4 - R^2 R_i^2}{2}\right) + \left(\frac{P' - \rho_o g}{4\mu_o}\right)\left(\frac{R_i^4}{4} - \frac{R_i^4}{2}\right) + \frac{(\rho_a - \rho_o) g R_i^4 \ln(R_i/R)}{4\mu_a}\right) \qquad (53)$$

From equations (50) and (52)

$$-\pi R_i^2 V_s = 2\left(\frac{P' - \rho_a g}{4\mu_a}\right)\left(\frac{R^4}{4} - \frac{R_i^4}{4} - \frac{R^4}{2} + \frac{R^2 R_i^2}{2}\right) + \frac{2\pi(\rho_a - \rho_o) g R_i^2}{2\mu_a}\left(\frac{r^2}{2}\ln\frac{r}{R} - \frac{r^2}{4}\right)_{R_i}^{R}$$

$$-\pi R_i^2 V_s = \left(\frac{P' - \rho_a g}{8\mu_a}\right)(2R^2R_i^2 - R^4 - R_i^4) + \frac{\pi(\rho_a - \rho_o)gR_i^2}{\mu_a}\left(-\frac{R_i^4}{4} - \frac{R^2R_i^2}{4} - \frac{R_i^4}{2}\ln\frac{R_i}{R}\right)$$

$$-\pi R_i^2 V_s = \left(\frac{P' - \rho_a g}{8\mu_a}\right)(2R^2R_i^2 - R^4 - R_i^4) + \frac{\pi(\rho_a - \rho_o)g}{\mu_a}\left(\frac{R_i^4}{4} - \frac{R^2R_i^2}{4} - \frac{R_i^4}{2}\ln\frac{R_i}{R}\right) \qquad (54)$$

The sum of the right hand sides of equations (53) and (54) is zero. By defining the ratio R_i/R as ϕ and dividing through by $\pi R^4/8$, following equation is obtained.

$$0 = \frac{(P' - \rho_a g)(2\phi^4 - 2\phi^2)}{\mu_a} + \frac{(P' - \rho_o g)(-\phi^4)}{\mu_o} + \frac{4(\rho_a - \rho_o)g\phi^4\ln\phi}{\mu_a} + \frac{(P' - \rho_a g)(2\phi^2 - 1 - \phi^4)}{\mu_a} + \frac{(\rho_a - \rho_o)g(2\phi^4 - 2\phi^2 - 4\phi^4\ln\phi)}{\mu_a}$$

$$0 = \frac{(P' - \rho_a g)(\phi^4 - 1)}{\mu_a} + \frac{(P' - \rho_o g)(-\phi^4)}{\mu_o} + \frac{(\rho_a - \rho_o)g(2\phi^4 - 2\phi^2)}{\mu_a} \qquad (55)$$

$$0 = P'\left(\frac{\phi^4 - 1}{\mu_a} - \frac{\phi^4}{\mu_o}\right) + \frac{\rho_a g(1 - \phi^4 + 2\phi^4 - 2\phi^2)}{\mu_a} - \frac{\rho_o g(-\phi^4)}{\mu_o} - \frac{\rho_o g(2\phi^4 - 2\phi^2)}{\mu_a} \qquad (56)$$

$$P' = \frac{\frac{\rho_o g(-\phi^4)}{\mu_o} + \frac{\rho_o g(2\phi^4 - 2\phi^2)}{\mu_a} - \frac{\rho_a g(1 + \phi^4 - 2\phi^2)}{\mu_a}}{(\frac{\phi^4 - 1}{\mu_a} - \frac{\phi^4}{\mu_o})} \tag{57}$$

Let $\mu_a/\mu_o = \psi$

$$P' = \frac{-\rho_o g\phi^4\psi + \rho_o g(2\phi^4 - 2\phi^2) - \rho_a g(1 + \phi^4 - 2\phi^2)}{\phi^4 - 1 - \phi^4\psi} \tag{58}$$

$$P' - \rho_a g = \frac{-\rho_o g\phi^4\psi + \rho_o g(2\phi^4 - 2\phi^2) - \rho_a g(1 + \phi^4 - 2\phi^2)}{\phi^4 - 1 - \phi^4\psi}$$

$$- \frac{\rho_a g(\phi^4 - 1 - \phi^4\psi)}{\phi^4 - 1 - \phi^4\psi}$$

$$= \frac{-\rho_o g\phi^4\psi + \rho_o g(2\phi^4 - 2\phi^2) - 2\rho_a g\phi^4}{\phi^4 - 1 - \phi^4\psi}$$

$$+ \frac{2\rho_a g\phi^2 + \rho_a g\phi^4\psi}{\phi^4 - 1 - \phi^4\psi}$$

$$= \frac{(\rho_a - \rho_o)g\phi^4\psi + (\rho_a - \rho_o)g(2\phi^2)}{\phi^4 - 1 - \phi^4\psi}$$

$$+ \frac{(\rho_a - \rho_o)(-2\phi^4 g)}{\phi^4 - 1 - \phi^4\psi}$$

$$= (\rho_a - \rho_o)g\,(\frac{\phi^4\psi + 2\phi^2 - 2\phi^4}{\phi^4 - 1 - \phi^4\psi}) \tag{59}$$

By substituting equation (59) into (54)

$$-\pi R_i^2 V_s = \frac{\pi(\rho_a - \rho_o)g(\phi^4\psi + 2\phi^2 - 2\phi^4)(2R^2R_i^2 - R^2 - R_i^4)}{8\mu_a(\phi^4 - 1 - \phi^4\psi)}$$

$$+ \frac{\pi(\rho_a - \rho_o)g}{\mu_a}\left(\frac{R_i^4}{4} - \frac{R^2R_i^2}{4} - \frac{R_i^4}{2}\ln\frac{R_i}{R}\right) \qquad (60)$$

Multiplying by $-8\mu_a/(\pi(\rho_a - \rho_o)gR_i^2R^2)$ to make both sides dimensionless,

$$\frac{8\mu_a V_s}{(\rho_a - \rho_o)gR^2} = -\frac{(\phi^4\psi + 2\phi^2 - 2\phi^4)(2 - \phi^{-2} - \phi^2)}{\phi^4 - 1 - \phi^4\psi}$$

$$- 8\left(\frac{\phi^2}{4} - \frac{1}{4} - \frac{\phi^2}{2}\ln\phi\right)$$

$$= \frac{(\phi^4(1 - \psi) + \phi^4 - 2\phi^2)(2 - \phi^{-2} - \phi^2)}{\phi^4(1 - \psi) - 1}$$

$$+ 2(1 - \phi^2) + 4\phi^2\ln\phi \qquad (61)$$

For the special case $\psi = 1$ (liquids of equal viscosity),

$$\frac{8\mu_a V_s}{(\rho_a - \rho_o)gR^2} = (2\phi^2 - \phi^4)(2 - \phi^{-2} - \phi^2) + 2$$

$$- 2\phi^2 + 4\phi^2\ln\phi$$

$$= \phi^6 - 4\phi^4 + 3\phi^2 + 4\phi^2\ln\phi \qquad (62)$$

From equation (56), for $\psi = 1$

$$0 = -(P' - \rho_a g) + (\rho_a - \rho_o) g(\phi^4 - 2\phi^2) \qquad (63)$$

It can be seen that as $\phi \to 1$, the pressure gradient is simply the organic phase hydrostatic gradient $\rho_o g$ and as $\phi \to 0$, the gradient is $\rho_a g$ as expected.

If the flow is solely determined by viscous forces, the value of ϕ would be such that the flow rates of each phase would be a maximum. This maximum for the case $\psi = 1$ can be obtained by differentiation of equation (62) and occurs at $\phi = 0.562$. It also follows that the maximum slug velocity would be

$$V_{smax} = 0.0185 R^2 (\rho_a - \rho_o) g / \mu_a \qquad (64)$$

Typically, for R = 0.5 cm, $(\rho_a - \rho_o) = 0.2$ g/mL, and $\mu_a = 0.01$ g/cm.s, $V_{smax} = 90.7$ cm/s

Observation indicates much lower values of V_s due to inertial and interfacial tension effects at the nose of the slug. Therefore, equation (61) must be used to estimate ϕ from the measured value of V_s. A plot of equation (61) over the range of experimental interest is given in figure 24.

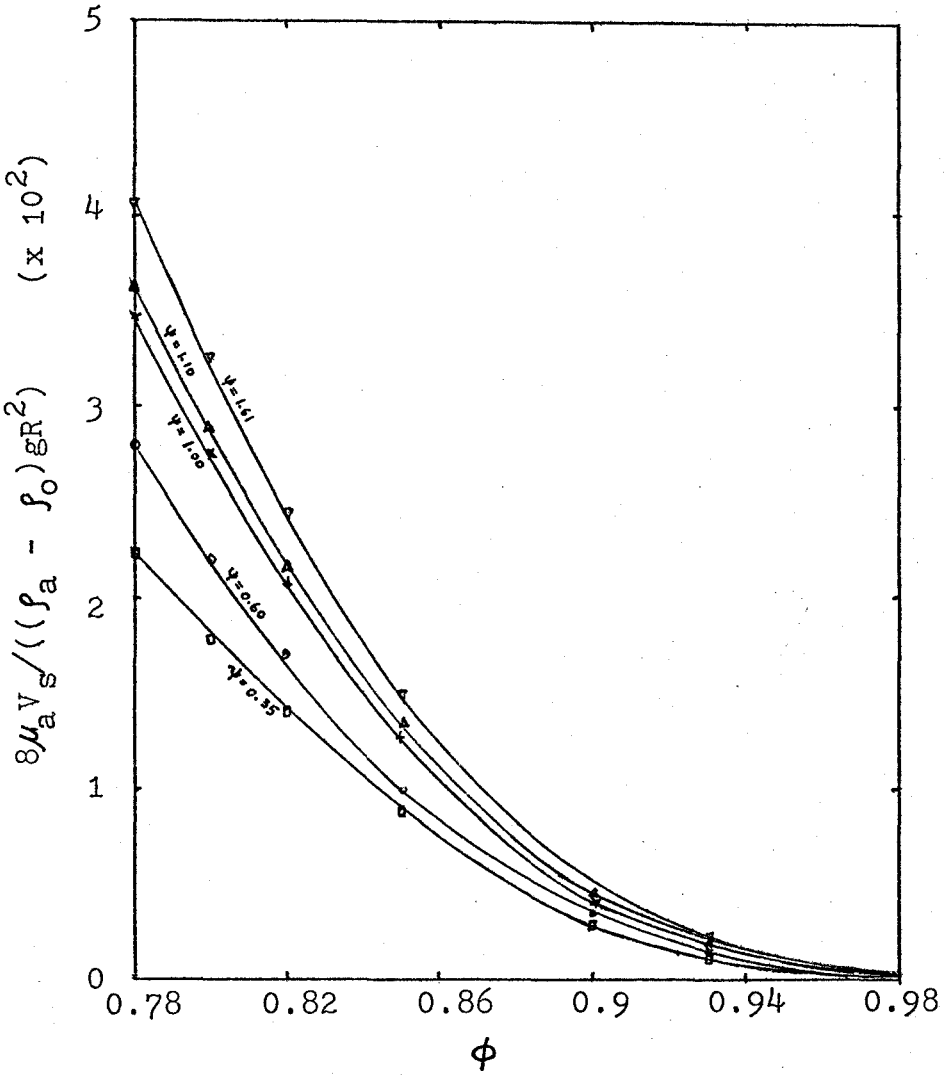

Figure 24. Velocity-ϕ plot for a slug rising through stagnant liquid

6.4. Solution for a stationary slug suspended in flowing liquid

The solution for a stationary slug is similar to that for a rising slug, except that the slug rising velocity V_s in this case is replaced by the slug's superficial velocity V_f which is the ratio of volumetric flow rate of flowing liquid to the tube cross-section area. The volumetric flow rate is a measured value, so is the superficial velocity of a slug.

Since the slug is stationary, from equation (51):

$$\pi R_i^2 V_s = \int_0^{R_i} 2\pi r V_o dr = 0 \qquad (65)$$

$$0 = 2\pi\left(\left(\frac{P' - \rho_a g}{4\mu_a}\right)\left(\frac{R_i^4}{2} - \frac{R^2 R_i^2}{2}\right) + \left(\frac{P' - \rho_o g}{4\mu_o}\right)\left(\frac{R_i^4}{4} - \frac{R_i^4}{2}\right)\right.$$

$$\left. + \frac{(\rho_a - \rho_o) g R_i^4}{4\mu_a} \ln\frac{R_i}{R}\right) \qquad (66)$$

Multiplying both sides by $8/\pi R^4$ and letting $R_i/R = \phi$,

$$0 = \left(\frac{P' - \rho_a g}{\mu_a}\right)(2\phi^4 - 2\phi^2) + \left(\frac{P' - \rho_o g}{\mu_o}\right)(\phi^4 - 2\phi^4)$$

$$+ \frac{4(\rho_a - \rho_o)}{\mu_a} g\phi^4 \ln\phi$$

$$= P'\left(\frac{2\phi^4 - 2\phi^2}{\mu_a} - \frac{\phi^4}{\mu_o}\right) - \frac{\rho_a g}{\mu_a}(2\phi^4 - 2\phi^2)$$

$$+ \frac{4(\rho_a - \rho_o)g\phi^4 \ln\phi}{\mu_a} \qquad (67)$$

$$P' = \frac{-\frac{\rho_o g\phi^4}{\mu_o} + \frac{\rho_a g}{\mu_a}(2\phi^4 - 2\phi^2) - \frac{4(\rho_a - \rho_o)}{\mu_a} g\phi^4 \ln\phi}{(\frac{2\phi^4 - 2\phi^2}{\mu_a} - \frac{\phi^4}{\mu_o})} \qquad (68)$$

Let $\mu_a/\mu_o = \psi$

$$P' = \frac{-\rho_o g\phi^4\psi + \rho_a g(2\phi^4 - 2\phi^2) - 4(\rho_a - \rho_o)g\phi^4 \ln\phi}{(2\phi^4 - 2\phi^2 - \psi\phi^4)} \qquad (69)$$

$$P' - \rho_a g = \frac{(\rho_a - \rho_o)g\phi^4\psi - 4(\rho_a - \rho_o)g\phi^4 \ln\phi}{(2\phi^4 - 2\phi^2 - \psi\phi^4)} \qquad (70)$$

For the aqueous phase (compare equation (54)):

$$\pi R^2 V_f = \frac{(P' - \rho_a g)(2R^2R_i^2 - R^4 - R_i^4)}{8\mu_a}$$

$$+ \frac{\pi(\rho_a - \rho_o)g}{\mu_a}(\frac{R_i^4}{4} - \frac{R^2R_i^2}{4} - \frac{R_i^4}{2}\ln\frac{R_i}{R}) \qquad (71)$$

Multiplying both sides by $8\mu_a/(\pi R^4(\rho_a - \rho_o)g)$

$$\frac{8\mu_a V_f}{R^2(\rho_a - \rho_o)g} = \frac{(\phi^4\psi - 4\phi^4 \ln\phi)(2\phi^2 - 1 - \phi^4)}{(2\phi^4 - 2\phi^2 - \psi\phi^4)}$$

$$+ (2\phi^4 - 2\phi^2 - 4\phi^4 \ln\phi) \qquad (72)$$

For special case $\psi = 1$,

$$\frac{8\mu_a V_f}{R^2(\rho_a - \rho_o)g} = \phi^4 - 2\phi^2 + \frac{\phi^2 - 4\phi^2 \ln\phi}{2 - \phi^2} \qquad (73)$$

When ϕ is zero or one, the slug superficial velocity is zero which is expected.

With a known value of slug superficial velocity, the ϕ value can be estimated from figures 25 and 26 which are plotted from equation (72). The velocity profiles of stationary slugs of 1-butanol, 1-pentanol and methyl isobutyl ketone are also plotted in figures 27 to 29 by using the equations (49) and (50) with the appropriate values of P' and ϕ for these systems.

A simple computer program is also prepared to find the interfacial radius ratio ϕ and interfacial velocity V_i, given the slug superficial velocity V_f. The program is illustrated in figure 30 with results in table 14.

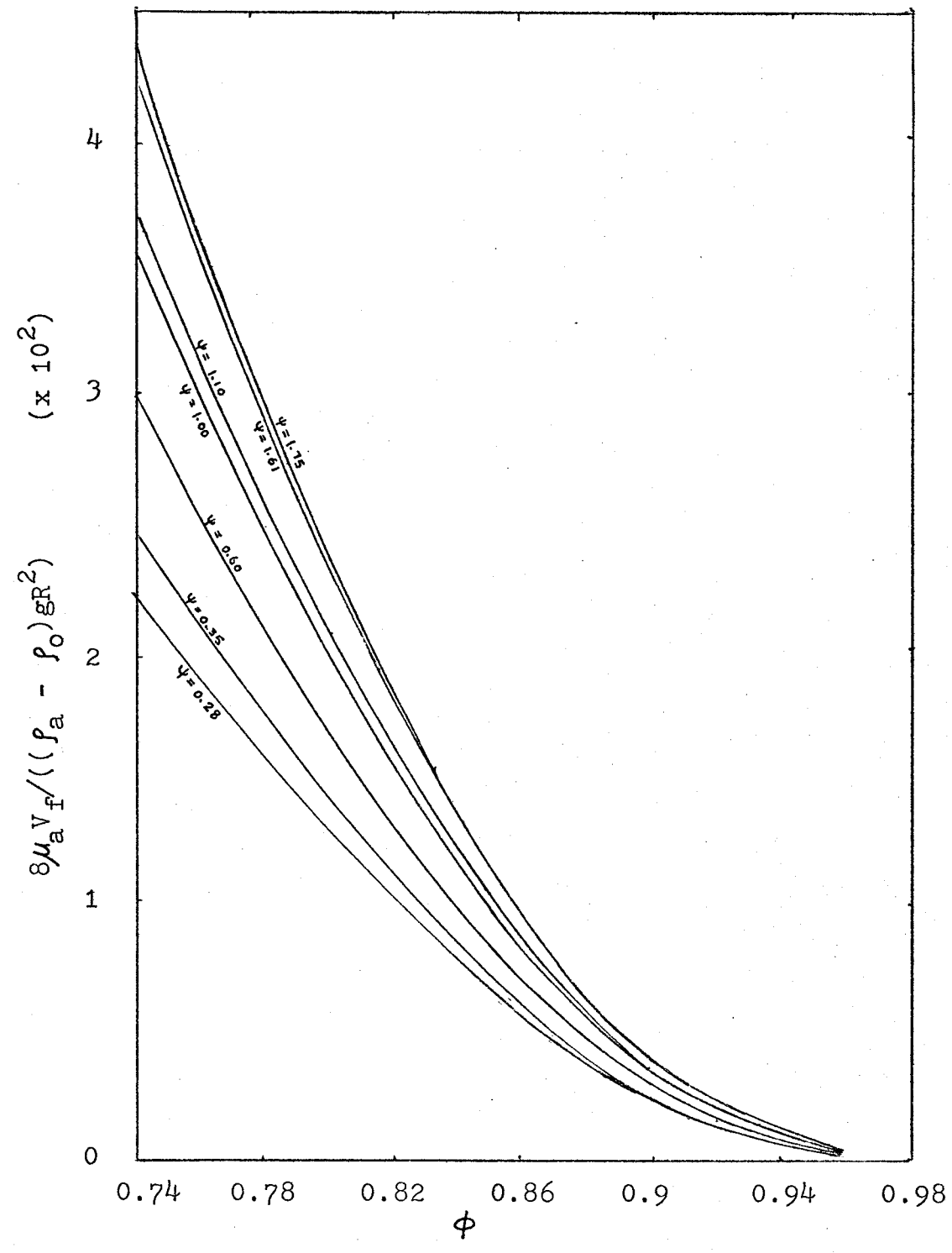

Figure 25. Velocity-ϕ plot for a stationary slug

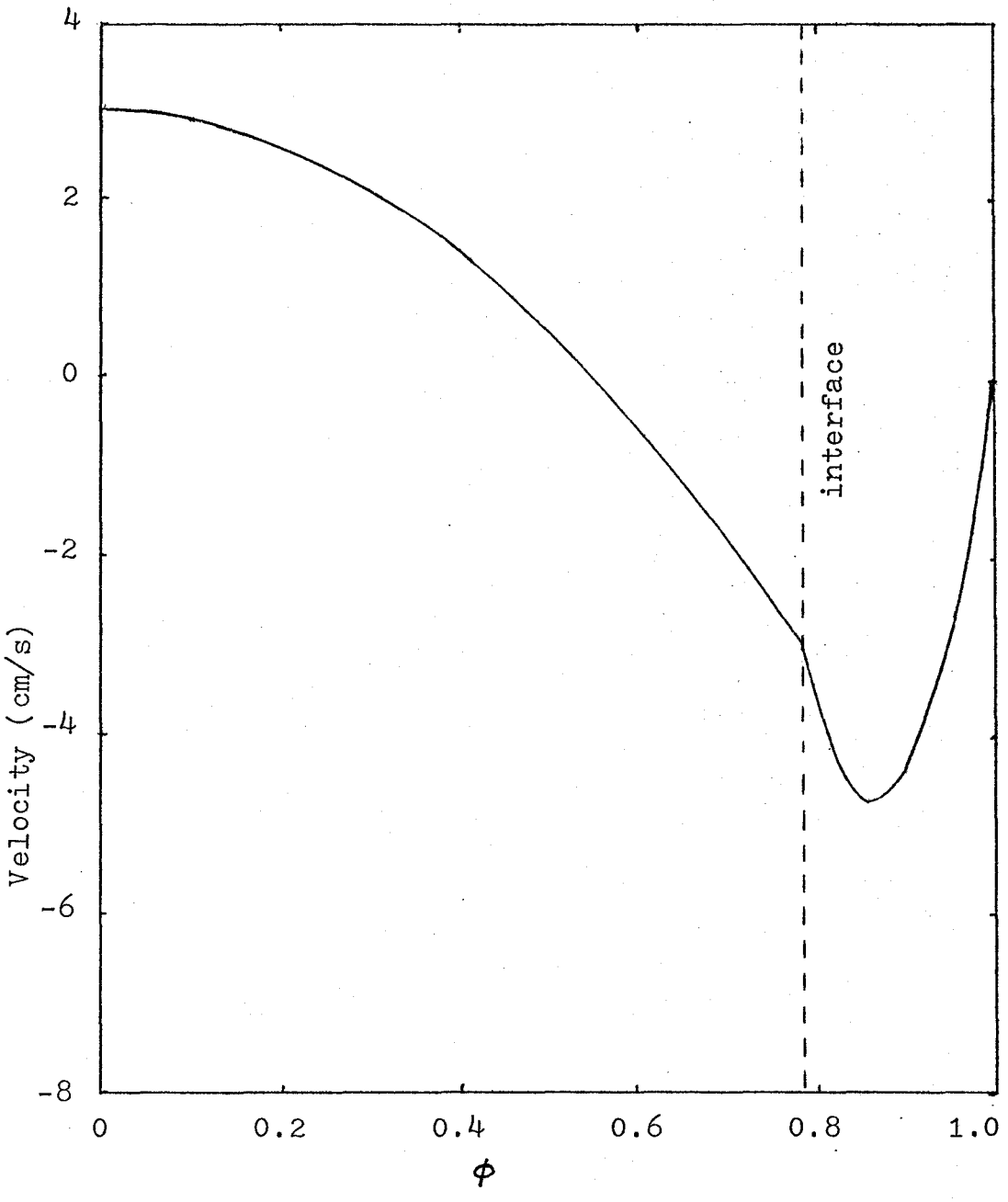

Figure 26. Velocity profile of a stationary slug (1-butanol)

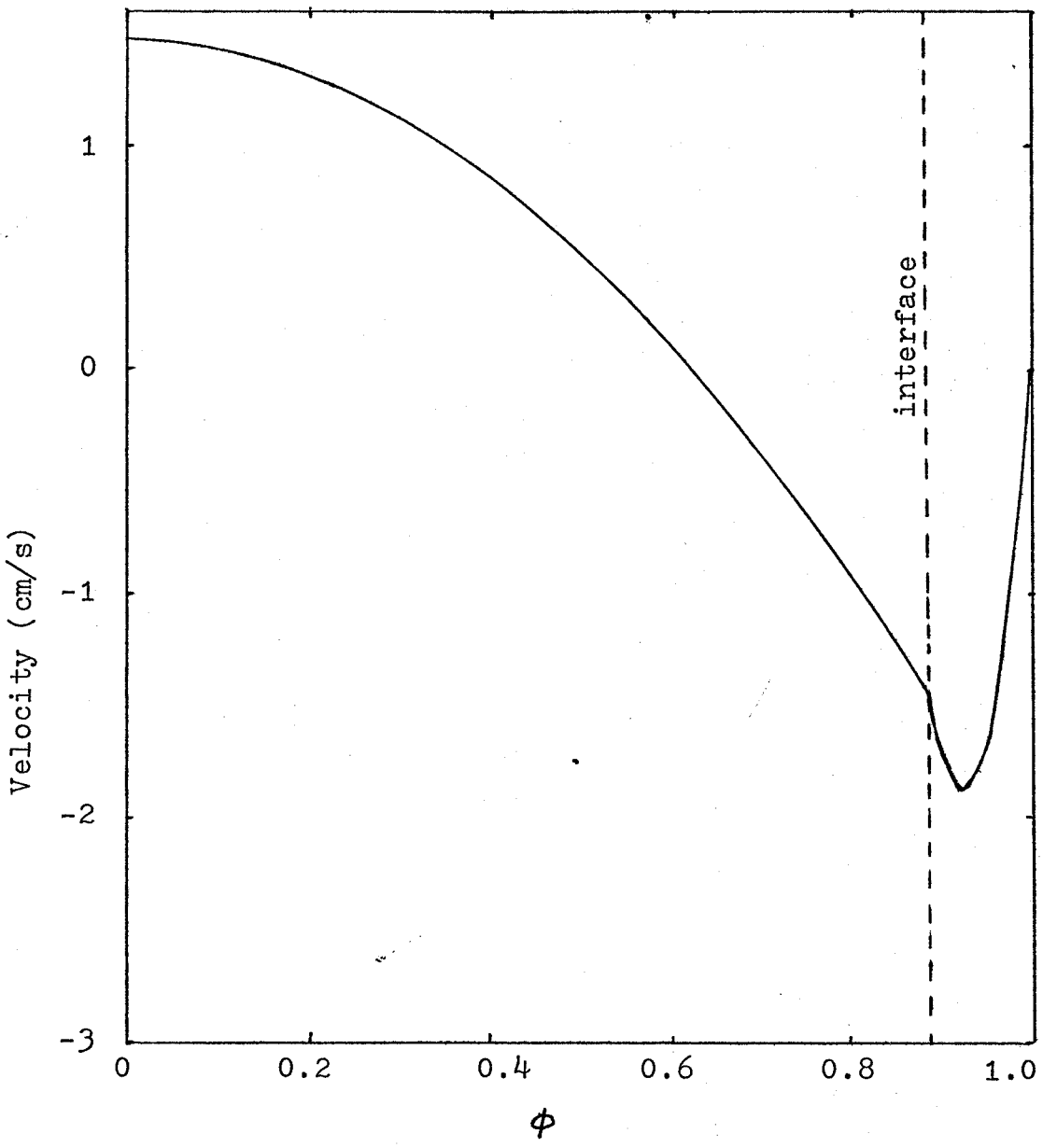

Figure 27. Velocity profile of a stationary slug (1-pentanol)

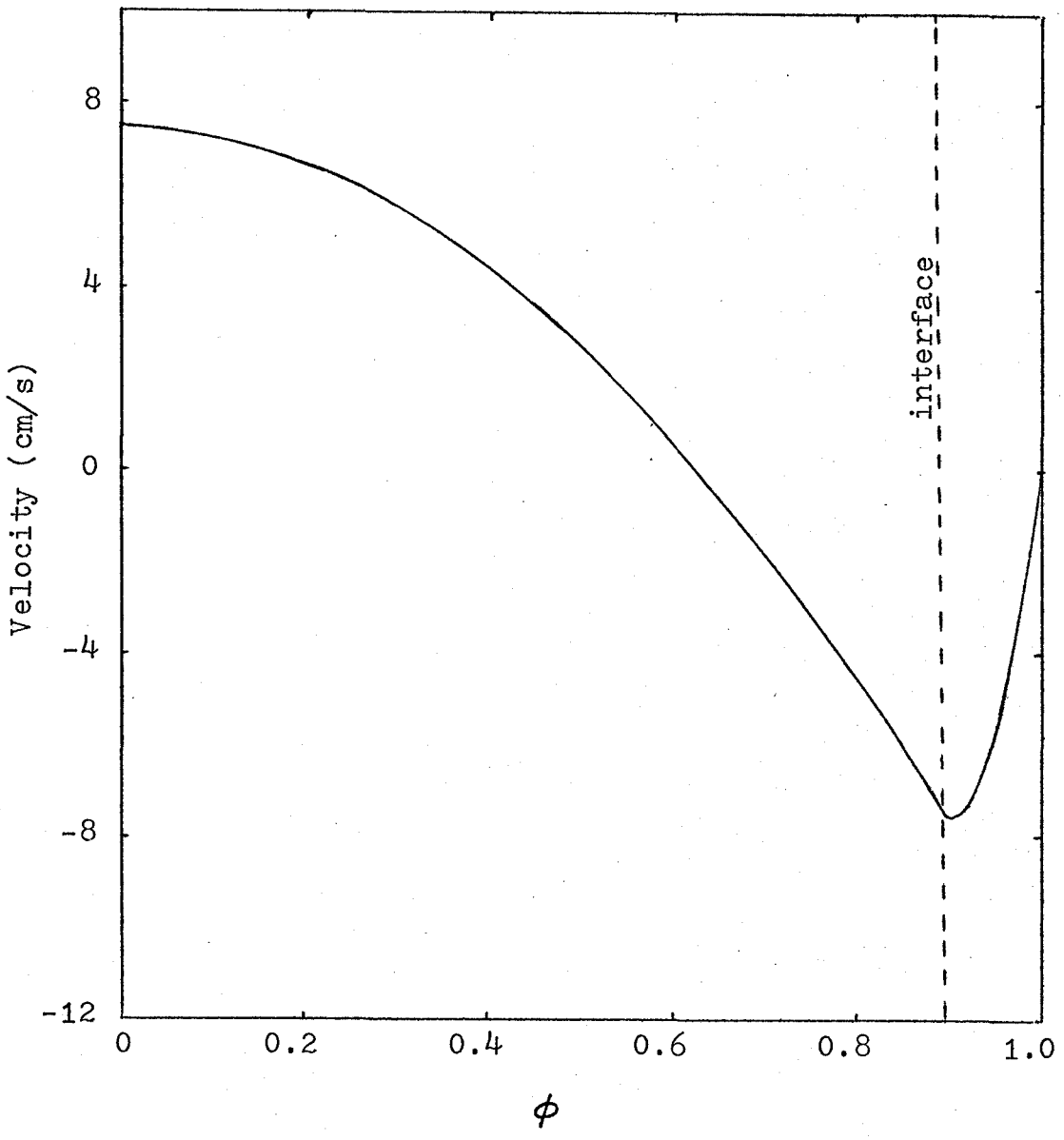

Figure 28. Velocity profile of a stationary slug (methyl iso-butyl ketone)

```
      PROGRAM TST (INPUT,OUTPUT,TAPE5=INPUT,TAPE6=OUTPUT)

C          THE INPUT DATA
C          RADIUS - RADIUS OF THE TUBE IN CM
C          DENA - DENSITY OF AQUEOUS PHASE IN G/ML
C          DENO - DENSITY OF ORGANIC PHASE IN G/ML
C          GRAV - GRAVITATIONAL CONSTANT IN CM/S**2
C          VISA - VISICOSITY OF AQUEOUS PHASE IN POISE
C          Q - VISICOSITY RATIO OF AQUEOUS TO ORGANIC
C          VELS - SUPERFICIAL VELOCITY IN CM/S
C          XX - TOLERANCE OF INTERFACIAL RADIUS RATIO

      RADIUS=0.204
      DENA=1.000
      DENO=0.840
      GRAV=980.0
      VISA=0.010
      VELS=1.326
      Q=0.35
      EONO=8*VISA*VELS/((RADIUS**2)*(DENA-DENO)*GRAV)
      XX=0.00001
      A=2
      G=60
  100 G=G+A
      P=G/100
      AA=P**4*Q-4*P**4*ALOG(P)
      BB=2*P**2-1-P**4
      CC=2*P**4-2*P**2-Q*P**4
      DD=2*P**4-2*P**2-4*P**4*ALOG(P)
      EE=(AA*BB/CC)+DD
      IF(EE.EQ.EONO) GO TO 717
      IF(EE.LT.EONO) GO TO 715
      EG=EE
      PG=G
      GO TO 100
  715 IF((EONO-EE).LT.XX) GO TO 717
      EE=EG
      G=PG
      A=A/10
      GO TO 100
  717 CONTINUE
      WRITE(6,710) P
  710 FORMAT(#-#,#     THE INTERFACIAL RADIUS RATIO = #,
     .F10.6)
      A1=P**4*Q-4*P**4*ALOG(P)
      A2=2*P**4-2*P**2-Q*P**4
      PRESG=(DENA-DENO)*GRAV*A1/A2
      B1=PRESG*(P**2-1)/(4*VISA)
```

```
      B2=(DENA-DENO)*GRAV*P**2*ALOG(P)/(2*VISA)
      VELIN=RADIUS**2*(B1+B2)
      VR=VELIN/VELS
      WRITE(6,123) VELIN,VR
123   FORMAT(#-#,#     INTERFACIAL VELOCITY = #, F10.5,
     ,//,#      VELOCITY RATIO OF INTERFACIAL TO
     ,SUPERFICIAL = #, F10.5)
      STOP
      END
```

Figure 29. A computer program for estimating ϕ and V_i

Table 14. Computed values of ϕ and V_i for stationary slugs of 1-butanol, 1-pentanol and methyl iso-butyl ketone (MIBK)***

System	tube diameter (mm)	ρ_o*(g/mL)	μ_o*(μPa.s)	V_f**(cm/s)	ϕ	V_i#(cm/s)
1-butanol	4.08	0.84	2860	1.326	0.786	3.05
1-pentanol	4.08	0.83	3520	0.287	0.888	1.44
MIBK	6.04	0.81	570	1.040	0.893	7.37

*The organic phase was saturated with water.

**The superficial velocity was measured experimentally.

#The interfacial velocities for 1-butanol, 1-pentanol and MIBK can also be observed from the velocity profiles in figures 26, 27 and 28 respectively.

***The density and viscosity of aqueous phase were assumed to be the same as that of water.

7. CALCULATION OF MASS TRANSFER RATES AND SHRINKAGE RATES FROM PENETRATION THEORY

7.1. Mass transfer rates

The contact time τ for the cylindrical interface is equal to L_s/V_i, where L_s is the slug length. From the Higbie penetration theory[1]

$$k_L = 2(D/(\pi\tau))^{\frac{1}{2}}$$

$$= 2(DV_i/(\pi L_s))^{\frac{1}{2}} \qquad (74)$$

Where k_L is the mass transfer coefficient and D is the diffusivity of the organic component in water. The mass transfer rate $\dot{m}$ is equal to the product of concentration driving force Δc, interfacial area A and mass transfer coefficient. Thus

$$\dot{m} = k_L A \Delta c$$

$$= k_L(2\pi R L_s \phi)\Delta c \qquad (75)$$

This expression neglects mass transfer at the front and rear ends of the slug, an approximation which is assumed valid for large slug length to diameter ratios.

7.2. Shrinkage rates

The mass transfer rate is also equal to the shrinkage rate:

$$\dot{m} = - \frac{d}{dt}(\pi R^2 \phi^2 L_s \rho') \tag{76}$$

Where ρ' is mass of pure organic liquid per unit volume of water-saturated organic phase. By balancing equations (75) and (76),

$$- \frac{d}{dt}(\pi R^2 \phi^2 L_s \rho') = k_L (2\pi R L_s \phi) \Delta c$$

$$-\pi R^2 \phi^2 \rho' \frac{dL_s}{dt} = k_L (2\pi R L_s \phi) \Delta c \tag{77}$$

$$\frac{dL_s}{dt} = - \frac{2 \Delta c k_L L_s}{\rho' R \phi} \tag{78}$$

If k_L were constant, the change of slug length with respect to time would be equal to the product of a constant K' and slug length. Thus

$$\frac{dL_s}{dt} = - K' L_s \tag{79}$$

By integration,

$$\ln(L_s/L_{so}) = - K' t \tag{80}$$

$$\ln L_s - \ln L_{so} = - K' t$$

$$\log L_s = - \frac{K' t}{2.303} + \log L_{so} \tag{81}$$

Where L_{so} is the length at time zero. If k_L is given

by equation (74), then from equation (78)

$$\frac{dL_s}{dt} = - \frac{4\Delta c}{\rho' R\phi}(DV_i L_s/\pi)^{\frac{1}{2}} \tag{82}$$

$$\frac{dL_s}{dt} = - KL_s^{\frac{1}{2}} \tag{83}$$

By integration,

$$L_s^{\frac{1}{2}} = L_{so}^{\frac{1}{2}} - Kt/2 \tag{84}$$

Therefore, the slope of a plot of $L_s^{\frac{1}{2}}$ versus time is

$$K/2 = \frac{2\Delta c}{\rho' R\phi}(DV_i/\pi)^{\frac{1}{2}} \tag{85}$$

8. MASS TRANSFER RESULTS AND DISCUSSION

8.1. Shrinkage rates

For the three organic liquids, the plots of slug length versus time are in figures 30 to 32, square root of slug length versus time are in figures 33 to 35 and logarithm of slug length versus time are in figures 36 to 38.

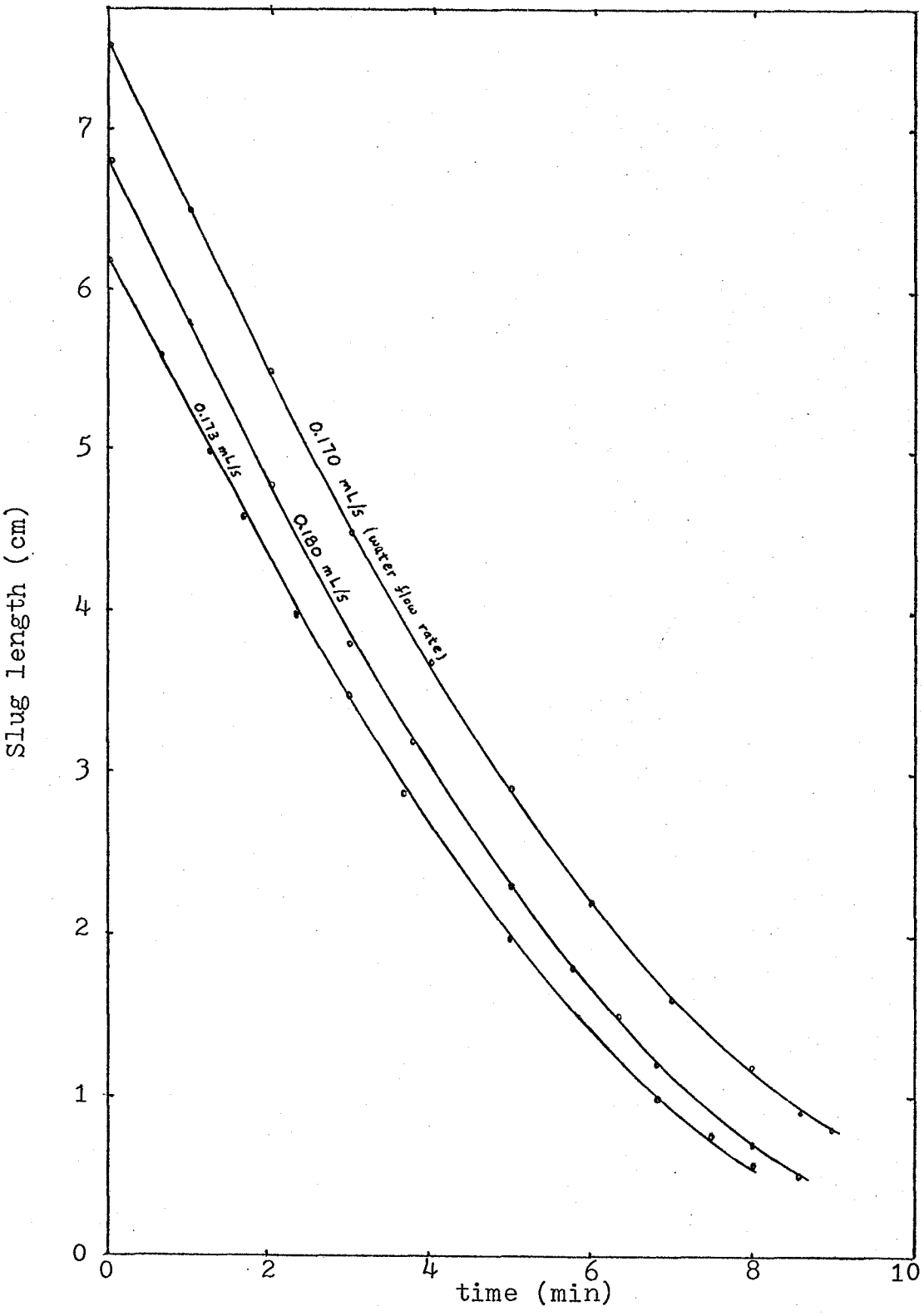

Figure 30. Slug length versus time (1-butanol)

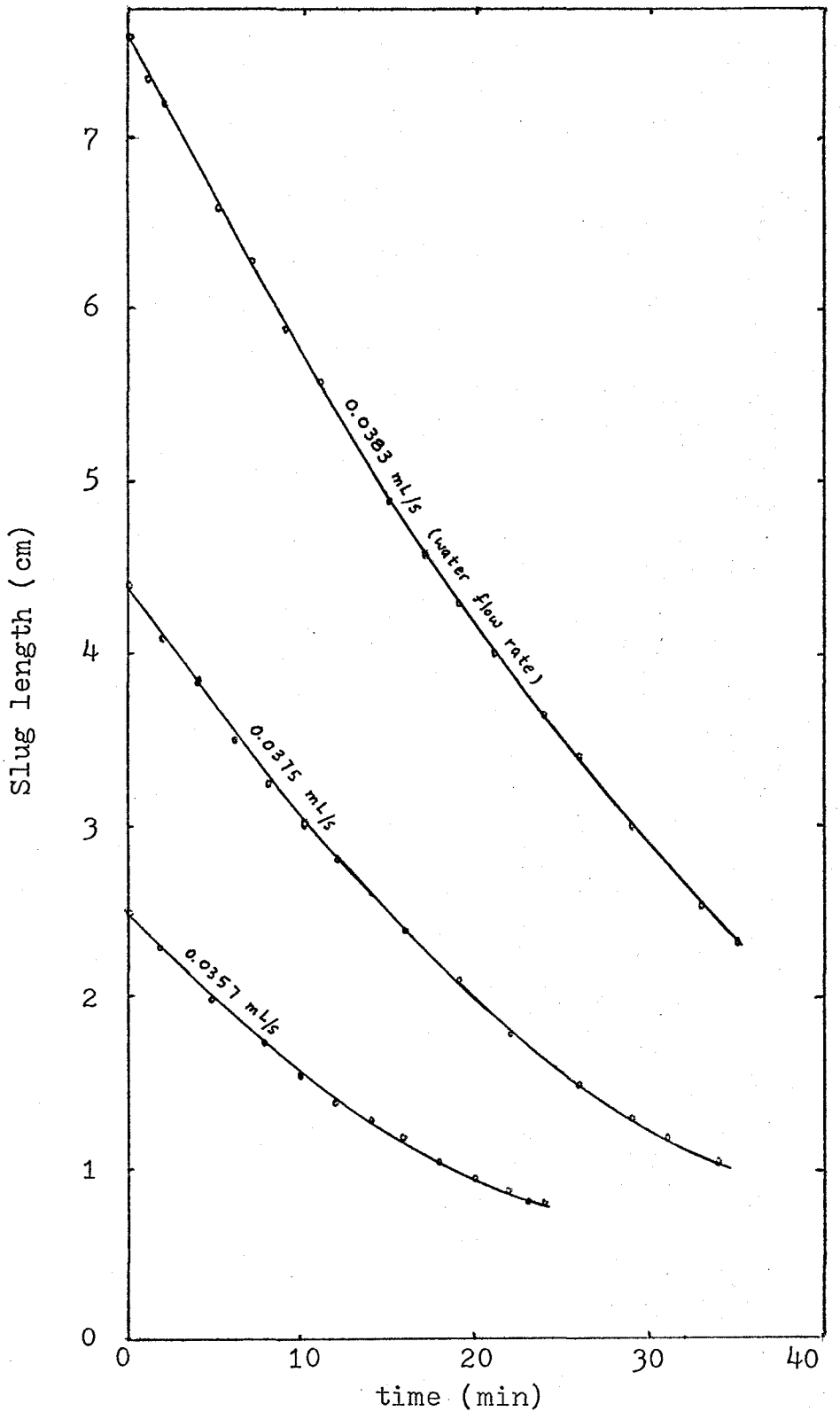

Figure 31. Slug length versus time (1-pentanol)

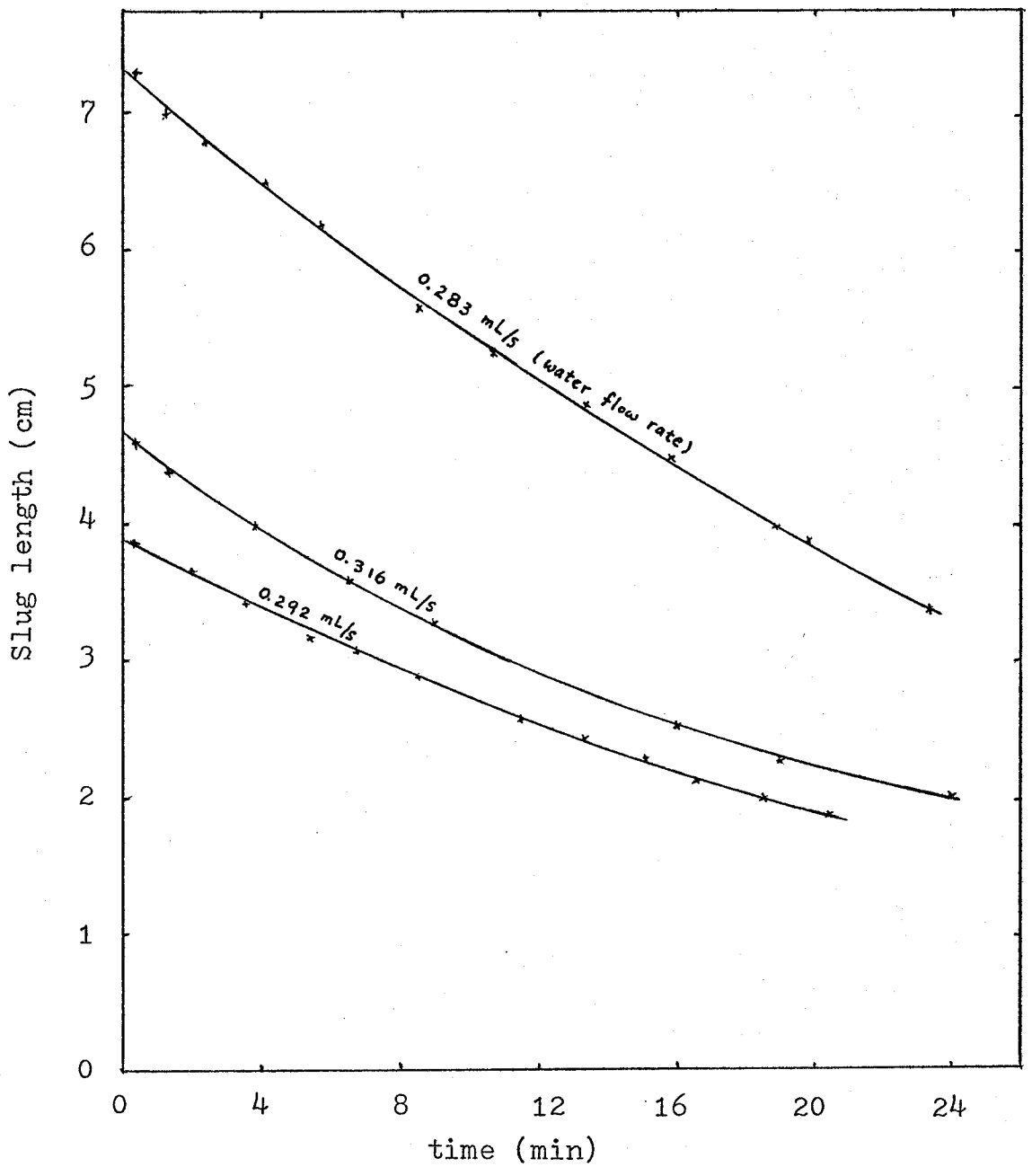

Figure 32. Slug length versus time (MIBK)

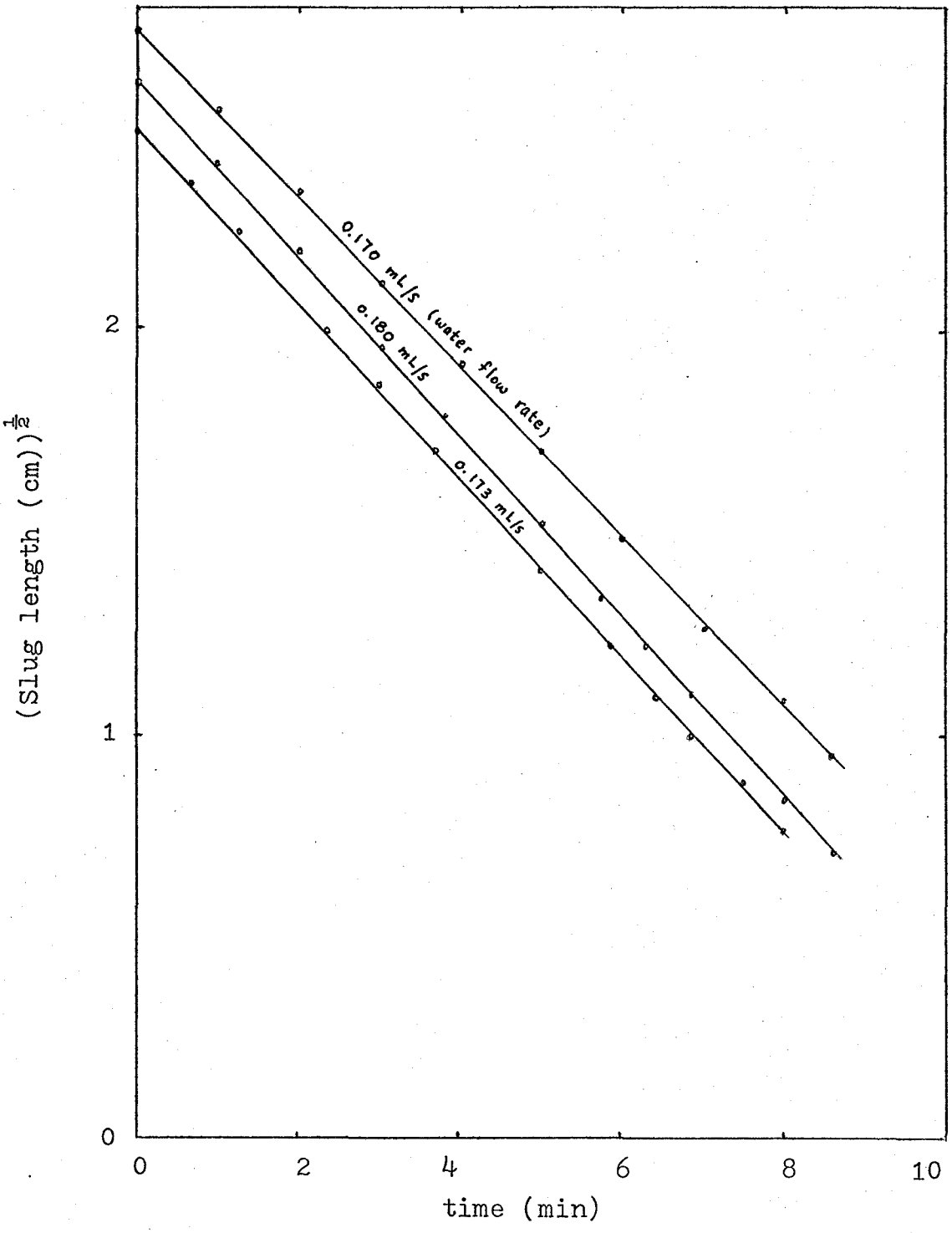

Figure 33. Square root of slug length versus time (1-butanol)

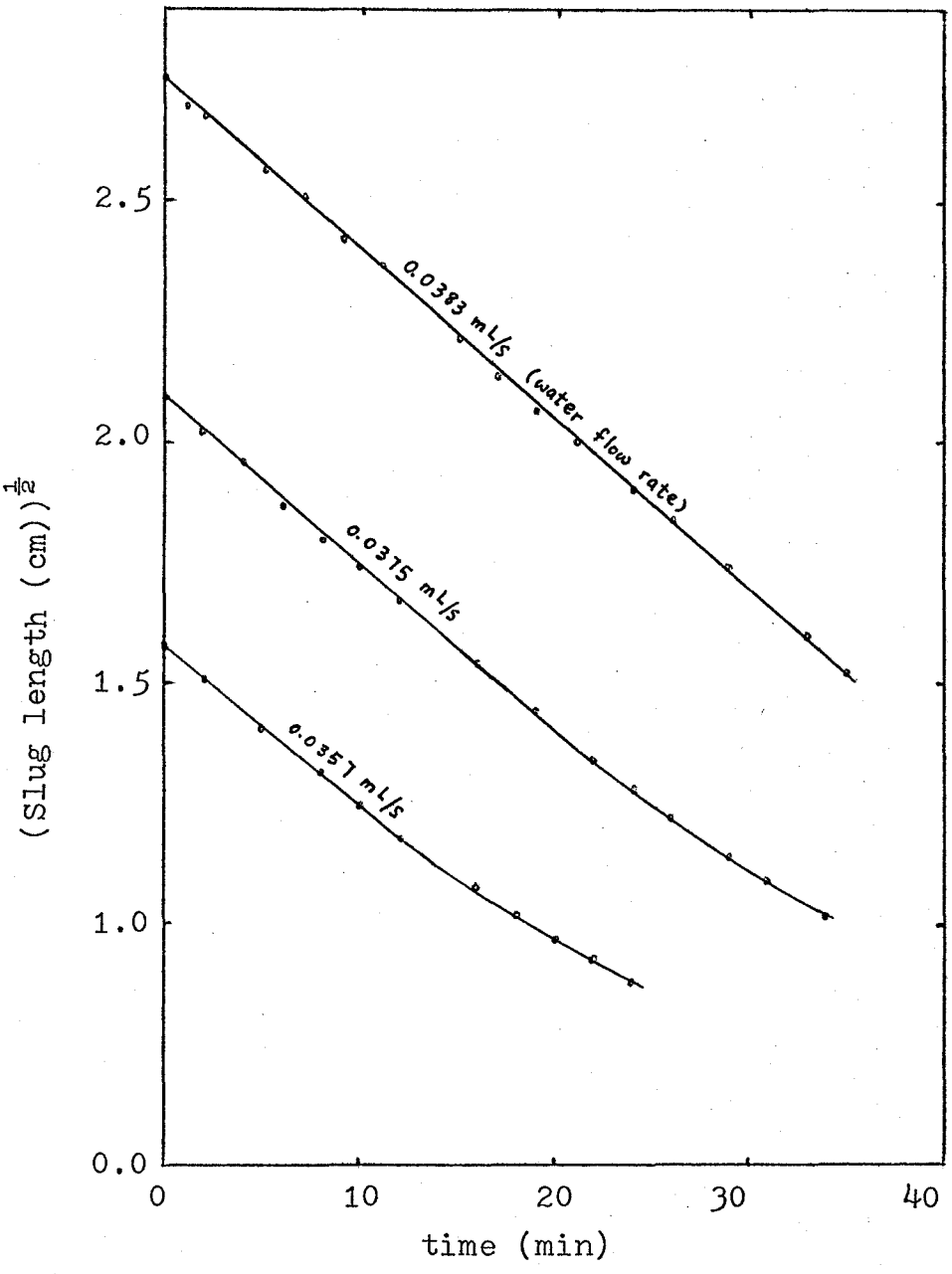

Figure 34. Square root of slug length versus time (1-pentanol)

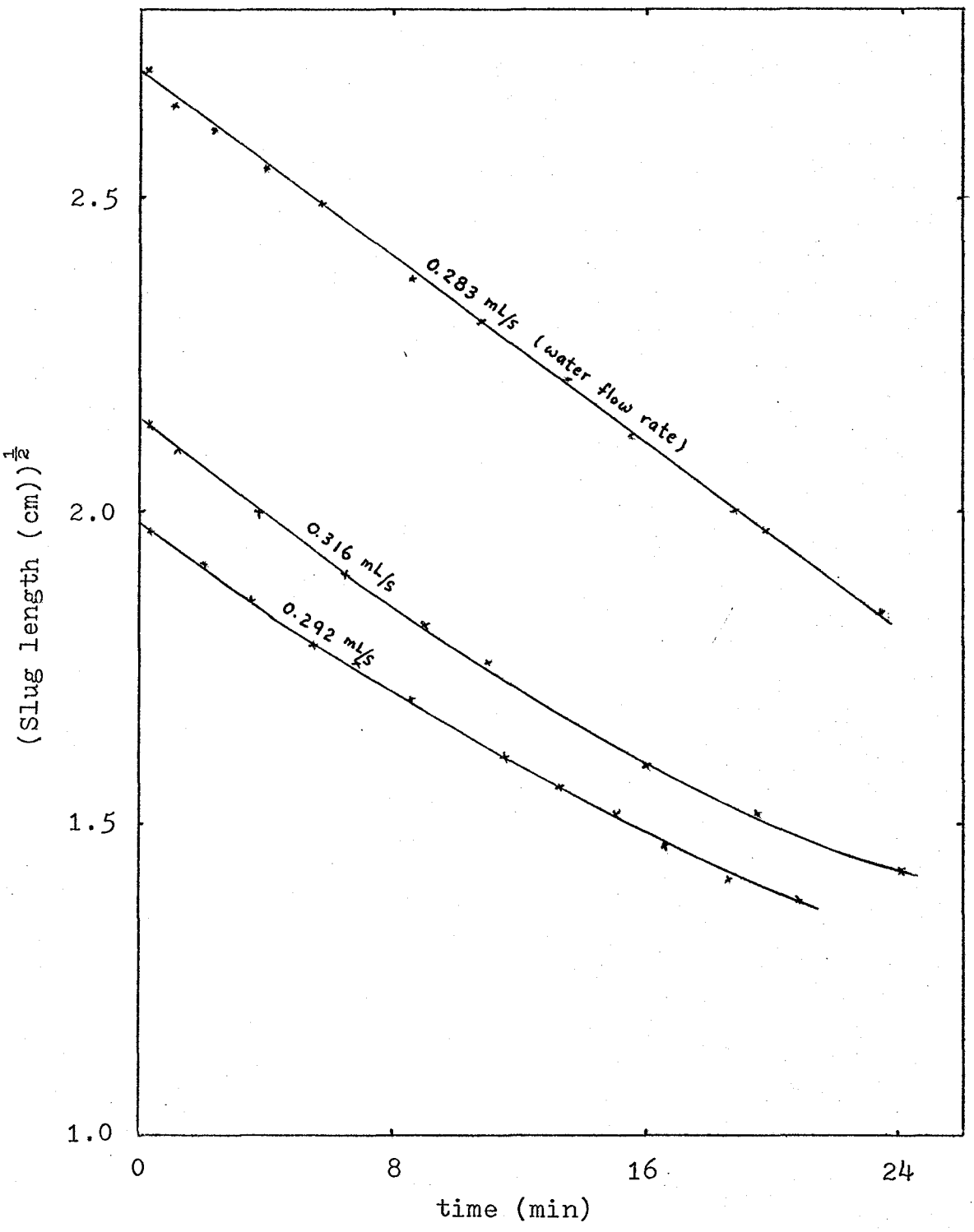

Figure 35. Square root of slug length versus time (MIBK)

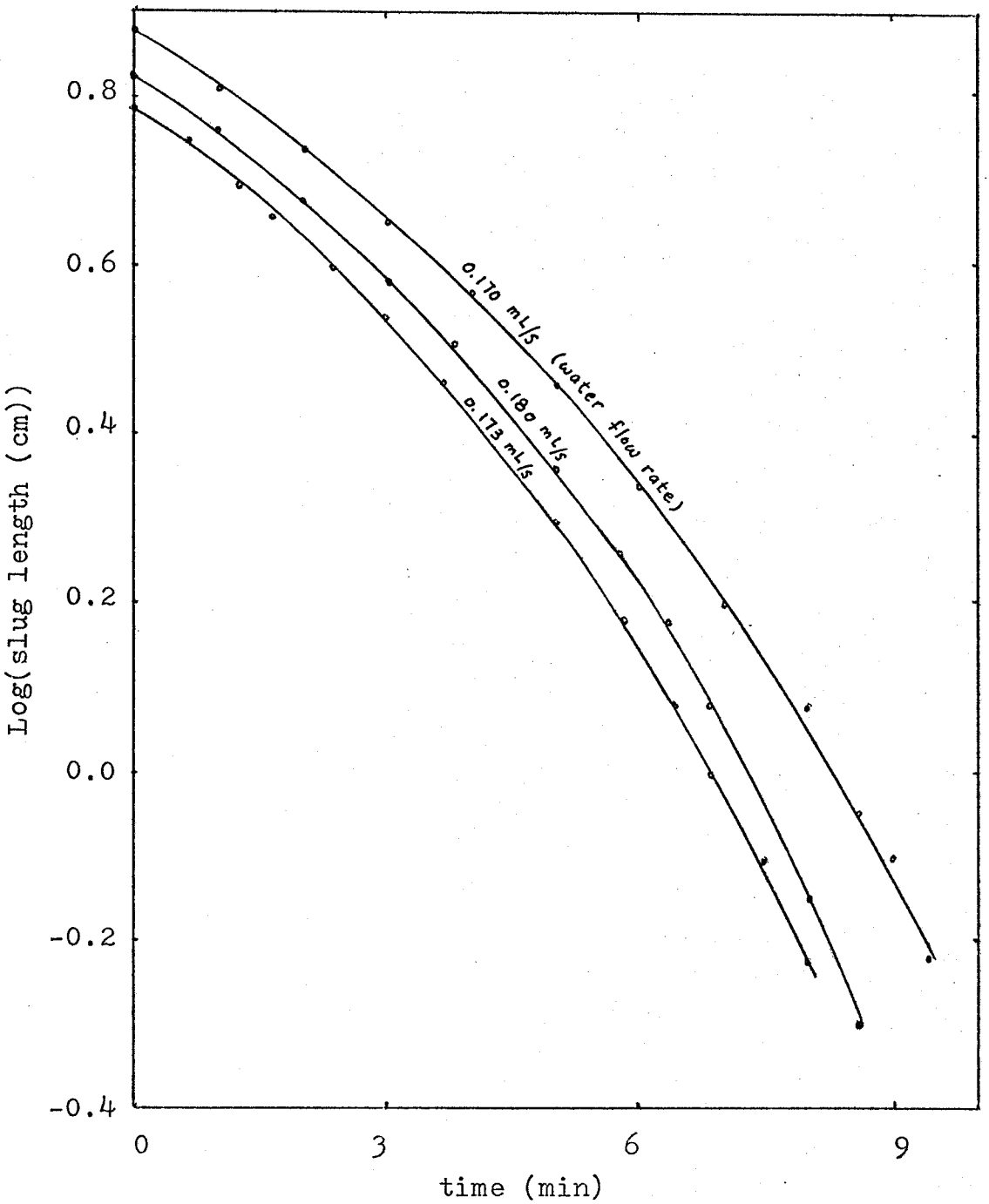

Figure 36. Logarithm of slug length versus time (1-butanol)

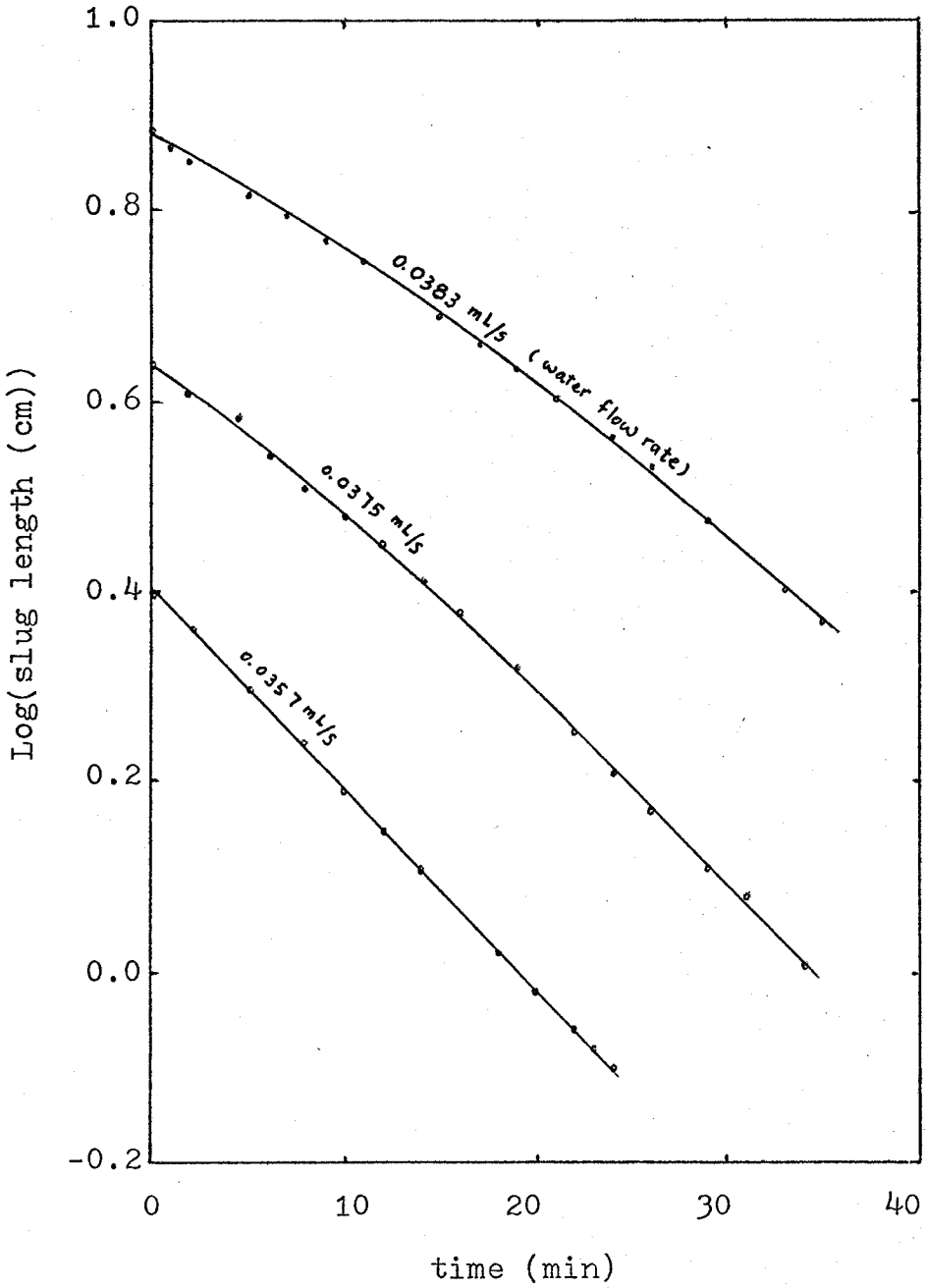

Figure 37. Logarithm of slug length versus time (1-pentanol)

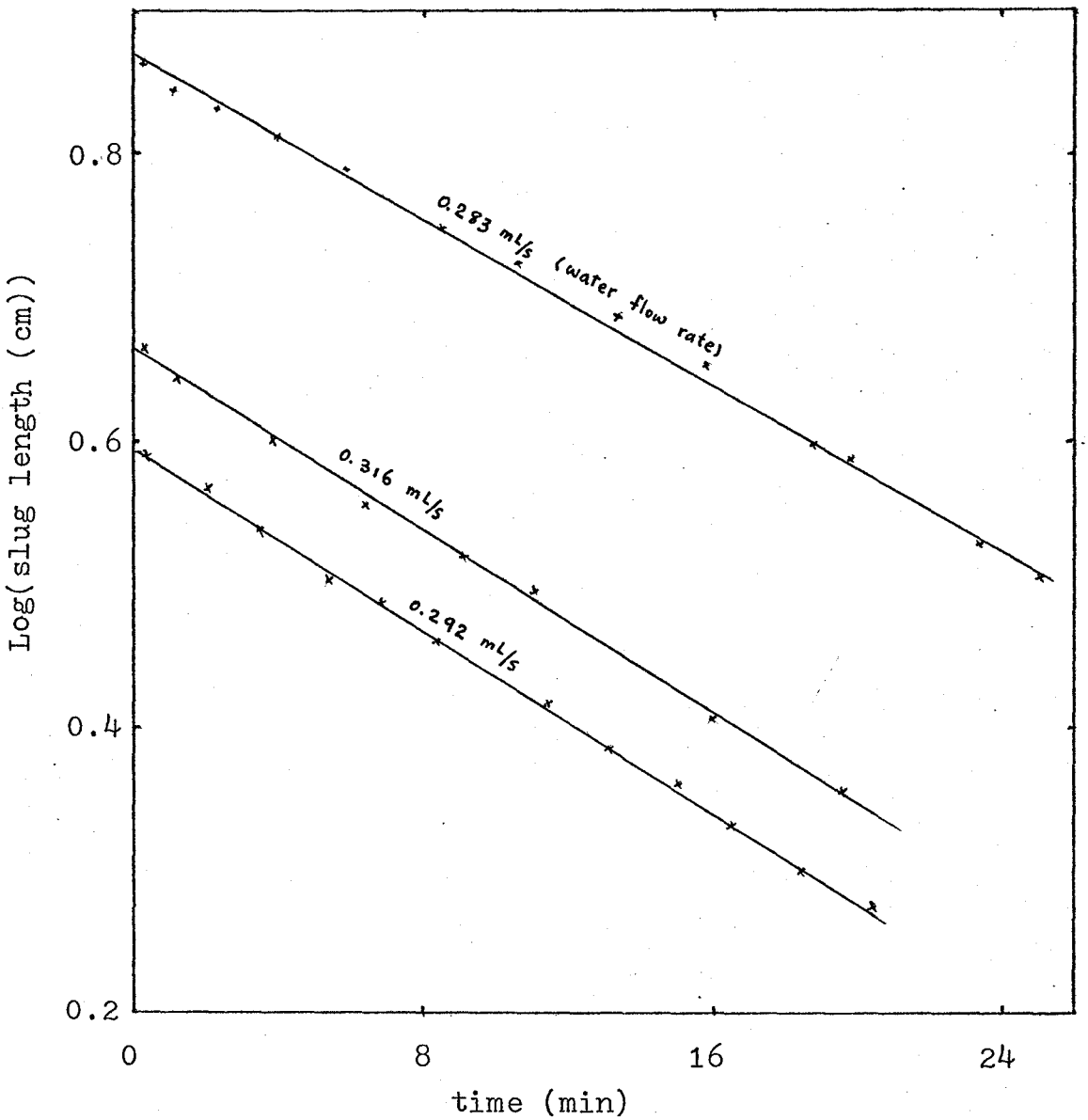

Figure 38. Logarithm of slug length versus time (MIBK)

8.2. Calculated mass transfer rates

Table 15

	1-Butanol	1-Pentanol	MIBK
Δc, g/mL	0.0786	0.0269	0.0207
ρ', g/mL	0.68	0.74	0.782
R, cm	0.204	0.204	0.302
ϕ (calc.)	0.786	0.888	0.893
V_f, cm/s	1.326	0.287	1.040
V_i, cm/s	3.05	1.44	7.37
D, cm^2/s			
(at inf. dil.)	0.96×10^{-5}	0.83×10^{-5}	0.77×10^{-5}
(at saturation)	0.65×10^{-5}	----	----
$K/2$, $cm^{\frac{1}{2}}/s$ (exptl.) 1st run	3.48×10^{-3}	5.90×10^{-4}	$*6.41 \times 10^{-4}$
2nd run	3.67×10^{-3}	5.85×10^{-4}	$*6.14 \times 10^{-4}$
3rd run	3.62×10^{-3}	5.67×10^{-4}	$*6.33 \times 10^{-4}$
Average	3.59×10^{-3}	5.81×10^{-4}	$*6.29 \times 10^{-4}$
$K/2$, $cm^{\frac{1}{2}}/s$ (calc.)			
(at inf. dil.)	4.4×10^{-3}	7.82×10^{-4}	8.21×10^{-4}
(at saturation)	3.62×10^{-3}	----	----

*It was estimated from initial slope.

8.3 Discussion (see table 15)

The molecular diffusivity of 1-butanol in water is quite strongly influenced by the concentration[16]. When the diffusivity at infinite dilution is used in the theoretical calculation, the rate constant K/2 found is about 20% higher than the observed value. However if the diffusivity at saturation is used in the theoretical calculation, the theoretical value is only 1% higher than the observed value. It is quite reasonable to use the diffusivity at saturation because the aqueous phase at the interface should be saturated with 1-butanol. Since there is a lack of experimental data on the diffusivities at saturation of 1-pentanol and methyl iso-butyl ketone, a comparison between theoretical values and experimental values cannot be precisely drawn. At infinite dilution, the theoretical K/2 values for both 1-pentanol and methyl iso-butyl ketone are about 25% higher than the observed values. The difference would obviously be reduced if lower molecular diffusivities were used in the calculations.

For the square root of slug length versus time plots in figures 34 and 35, the straight lines curve at the end. This would suggest that changes in the mass transfer mechanism may occur as shrinkage proceeds. The straight plot of logarithm slug length versus time in figure 38 may well indicate that the mass transfer coefficient for methyl iso-butyl ketone is constant throughout the operation, as illustrated in equation (81).

It is to be expected that the present theoretical approach becomes inadequate for shorter slugs, since it takes into account only the straight cylindrical part of the interface.

There are several other factors that could influence the mass transfer rate at the interface. The first is the contamination of the interface; surface active contaminants could accumulate at the end portion of the slug and reduce the contact time. The second is the non-cylindrical configuration at the end of the slug due to capillary effects (see figure 20). The third is that ripples begin to form when a long slug is used for the mass transfer operation and ripples would probably enhance the mass transfer rate.

Finally, it may be noted that the penetration distance of the solute from the interface, which is of the order of $(D\tau)^{\frac{1}{2}} = 4\times10^{-3}$ cm, corresponds to about 2% of the tube radius. It will be seen from figures 26 to 28 that there is some change in velocity across this distance, so that the penetration theory assumption of a constant contact time is only an approximation.

Despite these factors, it is believed that the mass transfer rates in liquid slugs would in general be predictable to within $\pm$ 10% using the penetration theory, provided the appropriate values of molecular diffusivity at saturation conditions are available.

9. CONCLUSIONS

1. The mass transfer device in this work is extremely simple and of low cost.
2. Two-phase slug flow in a tube of carefully chosen diameter gives a smooth interfacial area which can be calculated easily.
3. The mass transfer operation is performed in a capillary control regime, with the tube diameter slightly greater than the critical diameter for the liquid-liquid system being used.
4. The critical diameter of a slug can be measured using a tapered tube.
5. The Eotvos number relationship derived by Bretherton[22] can be used to estimate the surface or interfacial tension.
6. The interfacial radius ratio ϕ obtained from a rising slug is different from that for a slug held stationary by the downflow of liquid.
7. The experimental mass transfer results for 1-butanol show a good agreement with the Higbie penetration (within 1%).
8. The Higbie penetration theory overestimates by about 25% the mass transfer rates for 1-pentanol and methyl isobutyl ketone, but this is partly due to the necessity of using molecular diffusivity data for infinite dilution, no data for concentrated systems being available.

NOMENCLATURE

A	interfacial area, cm^2
b	film thickness, cm
c_1	mean curvature of the surface cm^{-1}
c	concentration difference between slug and aqueous phase, g/mL
d	tube diameter, cm
$d_{crit.}$	critical diameter, cm
D	molecular diffusivity, cm^2/s
D'	characteristic dimension of the duct cross section, cm
g	gravitational constant, 980 cm^2/s
h	height from the smaller end of a tapered tube, cm
k_L	mass transfer coefficient, cm/s
k_1, k_2, k_3	dimensionless constants
K	constant, $cm^{\frac{1}{2}}/s$
K'	constant, s^{-1}
L_s	slug length, cm
L_{so}	slug original length, cm
$\dot{m}$	mass transfer rate, g/s
N_{Ar}	dimensionless Archimedes number
N_{EO}	dimensionless Eotvos number
N_f	dimensionless inverse viscosity
P	dimensionless constant
P'	pressure gradient, $g/s^2.cm^2$

Q	dimensionless constant
r	radius, cm
R	tube radius, cm
R'	dimensionless constant
R_i	slug radius, cm
U_1, U_2	constants, cm/s
U_{1o}, U_{2o}	organic phase constants, cm/s
U_{1a}, U_{2a}	aqueous phase constants, cm/s
V	velocity, cm/s
V'	volume, cm^3
V_a	aqueous phase velocity, cm/s
V_b	flux, cm^2/s
V_i	interfacial velocity, cm/s
V_f	superficial velocity, cm/s
V_o	organic phase velocity, cm/s
V_s	slug velocity, cm/s
V_{smax}	maximum slug velocity, cm/s
x	height above some fixed level, cm
y	distance in horizontal direction, cm
y_1	the film thickness at which the surface tension departs from the bubble, cm
z	distance in vertical direction, cm
ρ	density of liquid, g/mL
ρ'	density of pure organic in wetted organic liquid, g/mL
ρ_a	aqueous phase density, g/mL
ρ_g	gas phase density, g/mL

ρ_1	density of continous phase, g/mL
ρ_o	organic phase density, g/mL
θ	angle, rad
η	dimensionless parameter
ξ	dimensionless parameter
μ	viscosity of liquid, g/cm.s
ρ_a	aqueous phase viscosity, g/cm.s
ρ_1	viscosity of continuous phase, g/cm.s
ρ_o	organic phase viscosity, g/cm.s
ϕ	dimensionless interfacial radius ratio
ψ	dimensionless aqueous to organic phase viscosity ratio
τ	contact time, s
σ	interfacial tension or surface tension, mN/m

REFERENCES

1. Higbie,R.: Trans. A.I.Ch.E., 31,365(1935)

2. Danckwerts.P.V. and A.M.Kennedy: Trans. Instn. Chem. Engrs., 32,S53(1954)

3. Roberts, D. and P.V. Danckwerts: Chem. Eng. Sci., 17, 961(1962)

4. Scriven,L.E. and R.L. Pigford: A.I.Ch.E.J., 4, 439(1958)

5. Lynn,S., J.R.Straatemeier, and H.K.Kramers: Chem. Eng. Sci., 4, part III,63(1955)

6. Govindan,T.S. and J.A.Quinn: A.I.Ch.E.J., 10,35(1964)

7. Ward,W.J. and J.A.Quinn: A.I.Ch.E.J., 11,1005(1965)

8. Ratcliff, G.A. and K.J.Reid: Trans. Inst. Chem. Engrs., 39, 423(1961)

9. Bakker,C.A.P., F.H.F.van Vlissingen and W.J.Beek: Chem. Eng. Sci., 22, 1349(1967)

10. Colburn,A.P. and D.G.Welsh: Trans. A.I.Ch.E., 38,179(1942)

11. Hodgman,C.D., R.C.Weast and S.M.Selby, 'Handbook of Chemistry and Physics', 42nd ed., 764-1283, The Chemical Rubber Publishing Company, 1960

12. Young,T.F. and W.D. Harkins: A.I.Ch.E., 12,857,No.5

13. Wellek,R.M., A.K.Agrawal and A.H.P.Skelland: A.I.Ch.E. Journal, 854,Sept(1966)

14. Perry,R.H. and C.H.Chilton,'Chemical Engineers' Handbook', 5th ed., 3-224, McGraw-Hill Book Company,1973

15. Wilke, C.R. and P.Chang: A.I.Ch.E.J., 1,264(1955)

16. Johnson,P.A. and A.L.Babb: Chem. Rev., 56,387(1956)

17. Wallis.G.B.,'One-Dimensional Two-Phase Flow', 285 -289, McGraw-Hill,1969

18. Dumitrescu,D.T.: Angew Math. Mech., 23,No.3,139(1943)

19. Davies,R.M. and G.I.Taylor: Proc.Roy.Soc.(London), 200, ser.A, 375 -390(1950)

20. White,E.T. and R.H.Beardmore: Chem. Eng. Sci., 17, 351 - 361(1962)

21. Wallis,G.B.: General Electric Company, Schenectady, N.Y.,Rept.62GL130,1962

22. Bretherton,F.P.: J. Fluid Mech., 10,166(1961)

23. Bolz,R.E. and G.L.Tuve,'Handbook of Tables for Applied Engineering Science', 2nd ed., 92 -93,1973